

**EVALUATION OF LOCAL OXYGEN CONSUMPTION IN  
HUMAN FLEXOR DIGITORUM SUPERFICIALIS MUSCLE  
BY NEAR INFRARED SPECTROSCOPY**

by

**Sinem Burcu ERDOĞAN**

B. S. in Chemical Engineering, Faculty of Engineering, Boğaziçi University, 2005

Submitted to the Institute of Biomedical Engineering  
in partial fulfillment of the requirements  
for the degree of  
Master of Science  
in  
Biomedical Engineering

Boğaziçi University  
September 2007

**EVALUATION OF LOCAL OXYGEN CONSUMPTION IN  
HUMAN FLEXOR DIGITORUM SUPERFICIALIS MUSCLE  
BY NEAR INFRARED SPECTROSCOPY**

**APPROVED BY:**

Assist.Prof.Dr. Ata AKIN .....  
(Thesis Advisor)

Assist.Prof.Dr. Can YÜCESOY .....

Assoc.Prof.Dr. Erdem KAŞIKÇIOĞLU .....

**DATE OF APPROVAL:** 10.09.2007

## ACKNOWLEDGMENTS

Upon completion of this M.Sc thesis, I would like to mention some names whom added a lot to my life experience and helped me set my goals for the future.

I would like to express my complete gratefulness to my thesis supervisor Dr. Ata Akin for his continuous support, friendly tolerance and encouragement throughout my studies. He has added a new dimension to my educational life and changed my whole vision for future by letting me in and helping me out of the Biomedical Engineering M.Sc program. I feel so privileged to work with such an indulgent and open-minded instructor.

Another person whom I am profoundly thankful is Dr. Can Yücesoy. His mercy had no limits while proofreading my work and I won't forget his patience and friendly tolerance. It is certain that there is much to learn from these two wonderful instructors and I am ready for full commitment to their supervision as long as they accept me as a prentice to educate. They have revitalized the satisfaction that comes from the pursuit of knowledge. Now, I even choose to pursue a Ph.D and perceive it both as a challenge and opportunity for personal growth.

I would also like to thank all my friends. They have always cheered up my life and without them life would not be as meaningful.

Last, I would like to thank my parents who have tried their best to make me happy in life and provided the best conditions in all aspects for my studies. Special thanks also goes to my little brother. His presence means a lot to me in life and even his presence is a wonderful feeling and a great source of happiness.

This work is dedicated to my parents.

## ABSTRACT

### EVALUATION OF LOCAL OXYGEN CONSUMPTION IN HUMAN FLEXOR DIGITORUM SUPERFICIALIS MUSCLE BY NEAR INFRARED SPECTROSCOPY

A strong relationship between mechanical and physiological conditions of skeletal muscle determines the force generated by that muscle. The aim of this study was to evaluate the relationship between local oxygen consumption and local force produced during isometric contractions at varying biomechanical conditions. Another aim of the study was to investigate the effect of relative position and absolute length changes on local energy consumption of flexor digitorum superficialis (FDS) muscle during isometric contractions performed at various muscle length and force levels.

Nine healthy male subjects performed sustained isometric handgrip exercise by continuously pressing on a hand dynamometer. The handgrip exercise was performed while the wrist is (i) maximally flexed, (ii) maximally extended and (iii) in neutral position. Local oxygen consumption ( $m\dot{V}O_2$ ) and time course of recovery ( $t_{rec}$ ) of FDS muscle were measured by functional near infrared spectroscopy (fNIRS).

$m\dot{V}O_2$  and  $t_{rec}$  were linearly related with force level up to 40% of maximal voluntary contraction force (MVC) at all wrist positions ( $p < 0.05$ ). At each force level,  $m\dot{V}O_2$  was observed to be lowest when the wrist was maximally extended ( $p = 0.0004$ ). Both parameters presented a decrease as the wrist was extended. The results imply that local energy consumption has a dependence on muscle relative position and length. It is suggested that myotendinous force transmission between a muscle and its surrounding structures might be a determinant of local of energy consumption.

**Keywords:** Near infrared spectroscopy, local oxygen consumption, isometric handgrip exercise.

## ÖZET

# İNSAN FLEXOR DIGITORUM SUPERFICIALIS KASININ BÖLGESEL OKSİJEN TÜKETİMİNİN YAKIN KIZILÖTESİ SPEKTROSKOPİ YÖNTEMİYLE İNCELENMESİ

İskelet kasının mekanik ve fizyolojik durumu arasındaki ilişki, ürettiği kuvveti belirlemede önemli rol oynar. Bu çalışmanın amacı, farklı biyomekanik koşullarda yapılan izometrik kasılmalar sırasında insan fleksör digitorum superficialis (FDS) kasının bölgesel oksijen tüketimi ile kuvvet üretimi arasındaki ilişkiyi incelemektir. Çalışmanın bir diğer amacı, farklı kuvvet seviyelerinde yapılan izometrik el sıkma egzersizi sırasında FDS kasının komşu sinerjist kaslara göre konumunun ve bu kasların mutlak boy değişimlerinin, bölgesel enerji tüketimine etkisini incelemektir.

Dokuz sağlıklı denek, el dinamometresini sürekli tutarak izometrik el sıkma egzersizi yaptı. El sıkma egzersizi, bilek (i) maksimal fleksiyonda (ii) maksimal ekstansiyonda ve (iii) nötral pozisyonda olmak üzere üç farklı bilek pozisyonunda yapıldı. FDS kasının bölgesel oksijen tüketimi ( $mVO_2$ ) ve egzersiz sonrası toparlama süreci ( $t_{rec}$ ) yakın kızılötesi spektroskopik yöntemiyle ölçüldü.

$mVO_2$  ve  $t_{rec}$ 'nin kuvvet seviyesiyle ilişkisinin maksimal istemli kasılma kuvvetinin % 40'ına kadar doğrusal olduğu bulundu ( $p<0.05$ ). Her kuvvet seviyesinde  $mVO_2$ 'nin bilek maksimal ekstansiyondayken en düşük olduğu görüldü ( $p=0.004$ ). İki parametre de bilek ekstansiyondayken azalma gösterdi. Sonuçlar, bölgesel enerji tüketiminin kasın komşu sinerjist kaslara göre konumunun ve bu kasların boy değişiminden etkilendiğine işaret etmektedir. Kasın komşu kas ve kasdışı yapılar arasındaki bağdokusal kuvvet iletiminin bu kasın enerji tüketimini belirlemede rol oynayabileceği önerilmiştir.

**Anahtar Sözcükler:** Yakın kızılötesi spektroskopik yöntemi, bölgesel oksijen tüketimi, izometrik el sıkma egzersizi.

## TABLE OF CONTENTS

ACKNOWLEDGMENTS . . . . .	iii
ABSTRACT . . . . .	iv
ÖZET . . . . .	v
LIST OF FIGURES . . . . .	viii
LIST OF TABLES . . . . .	ix
LIST OF SYMBOLS . . . . .	x
LIST OF ABBREVIATIONS . . . . .	xi
1. INTRODUCTION . . . . .	1
1.1 Motivation and Objectives . . . . .	1
1.2 Contribution of the Thesis . . . . .	2
1.3 Outline of the Thesis . . . . .	3
2. SKELETAL MUSCLE . . . . .	4
2.1 Histology of Skeletal Muscle . . . . .	4
2.2 Mechanism of Muscle Contraction . . . . .	7
2.3 Length Dependence of Force Production in Skeletal Muscle . . . . .	12
2.4 Myofascial Force Transmission . . . . .	15
2.5 Energy Metabolism in Skeletal Muscle . . . . .	15
2.6 Blood Flow and Oxygenation of Skeletal Muscle . . . . .	17
3. NEAR INFRARED SPECTROSCOPY . . . . .	19
3.1 Theoretical Basis of NIRS . . . . .	20
3.2 Application of NIRS in Exercise Physiology . . . . .	21
4. METHOD . . . . .	26
4.1 Subjects . . . . .	26
4.2 Experimental Protocol . . . . .	26
4.3 Data Collection . . . . .	28
4.4 Data Analysis . . . . .	29
4.4.1 Interpretation of the Signals . . . . .	31
4.4.2 Statistical Data Analysis . . . . .	31
5. RESULTS and DISCUSSION . . . . .	33

5.1	mVO <sub>2</sub> During Exercise . . . . .	33
5.1.1	The Relationship Between mVO <sub>2</sub> and the Level of Isometric Exercise . . . . .	33
5.1.2	The Effect of Wrist Position on the Relationship Between mVO <sub>2</sub> and the Level of Isometric Exercise . . . . .	35
5.2	Post-exercise Recovery Time ( $t_{rec}$ ) . . . . .	36
5.2.1	The Relationship Between $t_{rec}$ and the Level of Isometric Exercise. . . . .	36
5.2.2	The effect of altering wrist position on the relationship between $t_{rec}$ and the level of isometric exercise . . . . .	38
5.3	Interpretation of Results . . . . .	39
5.3.1	The Relationship Between mVO <sub>2</sub> and the Level of Isometric Exercise . . . . .	39
5.3.2	The Effect of Altering Wrist Position on mVO <sub>2</sub> of FDS Muscle . . . . .	40
5.3.3	The Relationship Between $t_{rec}$ and the Level of Isometric Exercise . . . . .	43
5.3.4	The effect of altering wrist position on $t_{rec}$ . . . . .	44
5.4	Limitations of the Study . . . . .	45
5.5	Recommendations for Future Work . . . . .	46
6.	CONCLUSION . . . . .	48
	APPENDIX A. mVO <sub>2</sub> and $t_{rec}$ Values for the Whole Set of Experiments . . . . .	50
	REFERENCES . . . . .	52

## LIST OF FIGURES

Figure 2.1	Schematic organization of a skeletal muscle.	5
Figure 2.2	Cross section of a muscle fiber.	6
Figure 2.3	Components of a sarcomere.	6
Figure 2.4	Neuromuscular junction and an alpha-motor unit.	8
Figure 2.5	The schematic diagram of skeletal muscle contraction.	9
Figure 2.6	Interaction between actin, myosin, $\text{Ca}^{+2}$ and ATP in relaxed and shortened muscle.	10
Figure 2.7	Structural arrangement of actin and myosin filaments at rest and during contraction.	11
Figure 2.8	Schematic representation of a sarcomere [1].	12
Figure 2.9	Force-length relationship of frog skeletal muscle sarcomere.	13
Figure 2.10	Sarcomere force-length relationship in frog, cat, and human skeletal muscles.	14
Figure 3.1	Wavelength dependence of light absorption in terms of skin penetration.	21
Figure 3.2	Absorption coefficients of various biological tissue components.	22
Figure 4.1	Schematic representation of the handgrip exercise.	27
Figure 4.2	The handgrip exercise while the wrist is maximally flexed.	27
Figure 4.3	Components of NIROXCOPE 301.	29
Figure 4.4	NIRS signals during a single exercise intensity.	30
Figure 5.1	Hb rise slope versus exercise intensity.	34
Figure 5.2	Length dependent $\text{O}_2$ consumption for FDS muscle.	35
Figure 5.3	$t_{rec}$ versus exercise level.	37
Figure 5.4	$t_{rec}$ at varying wrist positions.	38



**LIST OF TABLES**

Table 5.1	mVO <sub>2</sub> values derived from the Hb signal.	33
Table 5.2	Coefficients of regression equations and R <sup>2</sup> values.	34
Table 5.3	t <sub>rec</sub> measured from the Hb signal during exercise.	36
Table 5.4	Coefficients of regression equations and R <sup>2</sup> values.	38
Table A.1	mVO <sub>2</sub> values measured from the Hb signal	50
Table A.2	t <sub>rec</sub> measured from the Hb signal.	51

## LIST OF SYMBOLS

$\text{Ca}^{+2}$	Calcium ion
$\text{O}_2$	Oxygen
$\text{P}_i$	Inorganic phosphate
PCr	Phosphocreatine

## LIST OF ABBREVIATIONS

ACh	Acetylcholine
ADP	Adenosine diphosphate
ATP	Adenosine triphosphate
BOLD	Blood Oxygenation Level Dependent Signal
EDL	Extensor Digitorum Longus
EHL	Extensor Hallucis Longus
EPOC	Excess post-exercise oxygen consumption
FCR	Flexor carpi radialis muscle
FCU	Flexor carpi ulnaris muscle
FDS	Flexor digitorum superficialis
fNIRS	Functional near infrared spectroscopy
fMRI	Functional magnetic resonance imaging
Hb	Deoxy-haemoglobin
HbO <sub>2</sub>	Oxy-haemoglobin
[HbO <sub>2</sub> ]/[Hb]	Concentration of oxy/deoxy-haemoglobin
[Hb <sub>tot</sub> ]	Concentration of total haemoglobin
IMP	Intramuscular tissue Pressure
MRI	magnetic resonance imaging
MVC	Maximum voluntary contraction force
mVO <sub>2</sub>	Local oxygen consumption
NIRS	Near infrared spectroscopy
NIRS <sub>cws</sub>	Continous wave near infrared spectroscopy
OXY	Oxygenation
<sup>31</sup> P-MRS	Phosphorous magnetic resonance spectroscopy
t <sub>rec</sub>	Time course of recovery
TA	Tibialis Anterior

# 1. INTRODUCTION

## 1.1 Motivation and Objectives

Examining the changes in skeletal muscle oxygen consumption during a variety of exercise conditions has been a topic of interest for many years. Understanding the coupling of force generated and the local muscle oxygen consumption at rest and during exercise requires reliable quantitative measurements of local muscle oxygen consumption and blood flow. Near infrared spectroscopy (NIRS), a relatively new non-invasive optical technique; allows the simultaneous measurement of changes in intravascular and mitochondrial oxygenation and enables the study of local differences in muscle oxygen consumption and delivery.

External force generated by muscles depends on the level of electrical stimulation of the muscles and the mechanical and physiological conditions of the muscle. While the degree of electrical stimulation by the central nervous system can be measured by EMG, mechanical parameters and the condition of the muscle such as the force it generates, its length, and the internal muscular pressure can be quantified by stress, force and displacement sensors. Physiologic condition of a muscle depends on the local biochemistry (i.e. local oxygen consumption) and local blood delivery (i.e. blood flow and velocity) all of these factors are function of metabolism and vasculature dynamics.

Local oxygen consumption ( $m\dot{V}O_2$ ) in skeletal muscle can be used as a measure of energy metabolism to validate musculoskeletal models. However, the relationship between muscle oxygen consumption and external force, as a measure for muscle activity, is seldom investigated [2]. It is also likely that muscle length affects the relationship between external force generated and local oxygen consumption per unit time, but the extent of this effect has not yet been examined in vivo [3].

The aim of this study is to evaluate the relationship between local oxygen con-

sumption and local force produced during isometric contractions at varying biomechanical conditions. It has been shown that position of a muscle relative to its surroundings determines isometric muscle force in addition to absolute length of the structures involved in force generation [4]. So, another aim of the study is to investigate the effect of relative position and length changes on local energy consumption of FDS muscle during isometric contractions performed at varying length and force levels. A functional near infrared spectroscopy (fNIRS) device (NIROXCOPE 301) which measures local deoxy-hemoglobin (Hb) and oxy-hemoglobin (HbO<sub>2</sub>) concentration changes with respect to time, is used for the quantification of mVO<sub>2</sub> and time course of recovery ( $t_{rec}$ ) of human FDS muscle during sustained isometric handgrip exercise. Local energy consumption during exercise is evaluated by analyzing changes in mVO<sub>2</sub> and  $t_{rec}$  (i) with wrist position and (ii) exercise level represented as percentages of the maximal voluntary contraction force (% MVC).

## 1.2 Contribution of the Thesis

The major contribution of this thesis work is examining the effect of relative position and absolute length changes of FDS and adjacent synergist muscles on the relationship between local energy consumption and local force produced by this muscle during sustained isometric handgrip exercise. An experimental protocol is designed;

1. to assess the deoxygenation of FDS muscle during isometric force production at different wrist positions and contraction intensities;
2. to investigate whether changes in relative position and absolute length of a muscle and its adjacent synergist muscles affect local energy consumption, using the easily applicable non-invasive NIRS technique.

To date, there are no existing studies that have attempted to analyze length and relative position dependence of local energy consumption in human skeletal muscle with NIRS.

### 1.3 Outline of the Thesis

Chapter 1 introduces the thesis. A brief information about the skeletal muscle physiology and function is given in Chapter 2. Chapter 3 explains the NIRS modality and its applications in sports medicine. Chapter 4 provides a broad explanation on the design of experimental protocol and data analysis procedure. Results of the experiments are given in Chapter 5. A thorough interpretation of results, comparison with previous studies and recommendations for future work are also included in the subsections of this chapter. Finally, Chapter 6 mentions concluding remarks for the study.

## 2. SKELETAL MUSCLE

The human body contains approximately 660 skeletal muscles which make up about 40 % of total body weight. Skeletal muscles serve 3 important functions: (i) providing the means for human motion, (ii) force generation for performing both dynamic and static work and (iii) heat production for maintaining homeostasis of body temperature [5].

Skeletal muscles create movement by applying force to bones and joints; via contraction. They generally contract voluntarily although they can also contract involuntarily through reflexes.

### 2.1 Histology of Skeletal Muscle

Skeletal muscle is composed of a collection of muscle cells which are called **muscle fibers**. Muscle fibers are cylindrical, elongated cells with multiple nuclei. As illustrated in Figure 2.1, each muscle fiber is surrounded by a thin layer of connective tissue called the **endomysium**. Thousands of muscle fibers are wrapped by a thin layer of connective tissue, namely the **perimysium** to form fascicles. Groups of fascicles that join into a tendon at each end form the muscle belly [6].

Skeletal muscle fibers can be further divided into subcellular levels of organization. The cell membrane of a muscle fiber is called the **sarcolemma** and the cytoplasm is called the **sarcoplasm**. Sarcolemma does not only control what enters and leaves the cell, but also contains regulatory proteins that are influenced by hormones like epinephrine (adrenalin) and insulin. Skeletal muscle fibers contain an extensive network of tubular channels and vesicles that wraps around each myofibril. This system is called the **sarcoplasmic reticulum** and provides structural integrity to the cell. Figure 2.2 illustrates the cross section of a muscle fiber and its connective tissue wrappings.

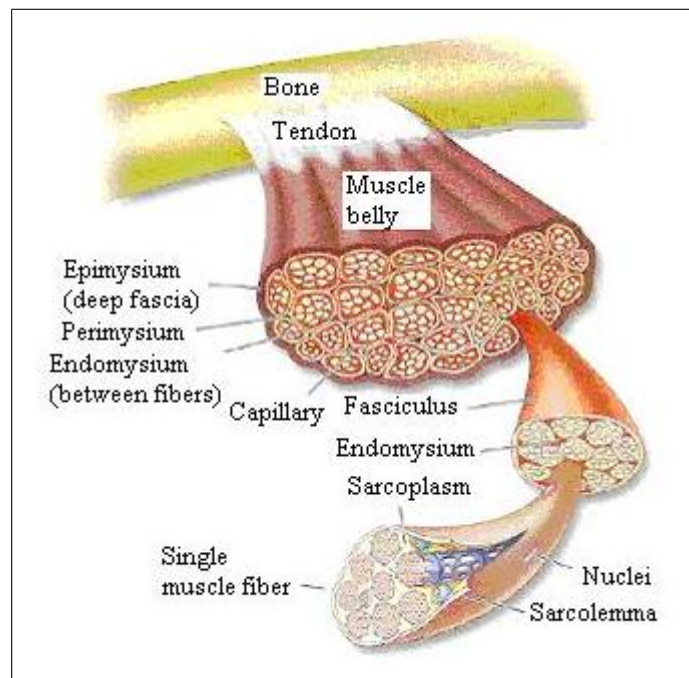


Figure 2.1 Schematic organization of a skeletal muscle [6].

Muscle fibers appear striated when examined using electron microscopy. The main intracellular structures are contractile and elastic proteins. The contractile units are called the **myofibrils** which contain even smaller subunits that lie parallel to the long axis of the multi-nucleated cell structure. Each myofibril is composed of several types of proteins including the contractile proteins **myosin** and **actin** and the regulatory proteins **tropomyosin** and **troponin**.

Myofibrils have a banded appearance created by a series of repeated units, called **sarcomeres**, which form the basic contractile unit of skeletal muscle. The ends of a sarcomere are marked by **Z (Zwischenscheiben) lines**. The **I (isotropic) band** lies on either side of the Z line and the **A (anisotropic) band** is found in the center of the sarcomere. The I band is composed of thin filaments which project from the Z line while the A band has thick filaments and overlapping thin filaments [6].

**Actin** is the protein that makes up the thin filaments of the muscle fiber. One actin molecule is actually a globular protein and multiple globular actin molecules polymerize to form long chains or filaments. **Myosin** is the protein that makes up the



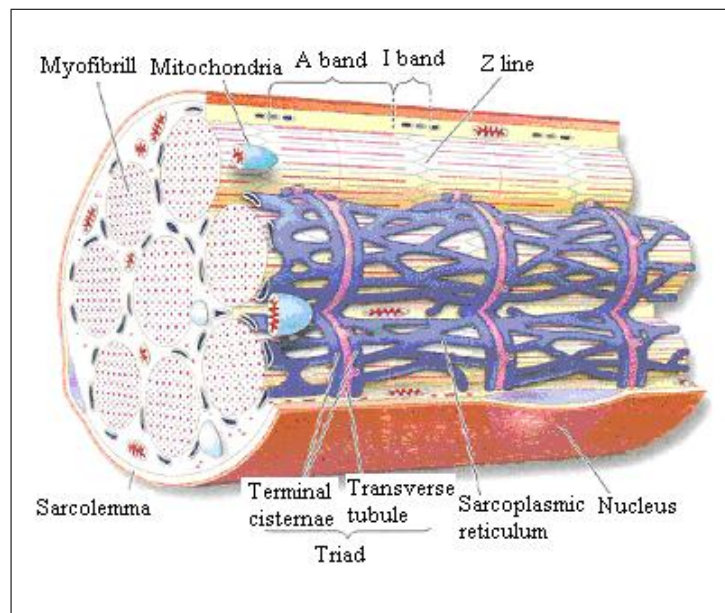


**Figure 2.2** Cross section of a muscle fiber [6].

thick filament of the myofibril. Each myosin molecule is composed of two heavy protein chains that intertwine to form a long coiled tail and a pair of heads. Actin and myosin filaments are arranged in parallel and connected by crossbridges. The **crossbridges** are the myosin heads that bind to the actin filaments. Each actin molecule has a single binding site for a myosin head.

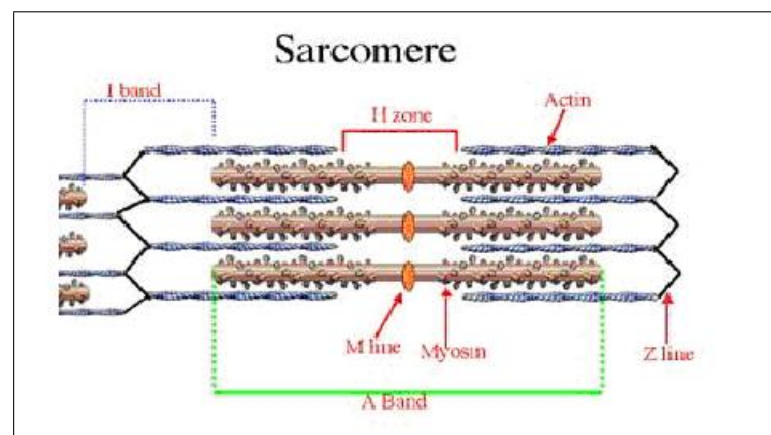


**Figure 2.3** The components of a sarcomere, the basic contractile unit [5].

In the relaxed state, a sarcomere has a large I band (thin filaments only) and an A band whose length is the length of the thick filament. The two Z disks at each end move closer together while the I band and H zone almost disappear. These are regions where actin and myosin do not overlap in resting muscle.

As the muscle contracts, the thick and thin filaments slide past each other, moving the Z disks of the sarcomere closer together. During the relaxed state, thin filaments in a sarcomere form the I band only and thick filaments make up the A band. The two Z disks at each end move closer together while the I band and H zone almost disappear. These are regions where actin and myosin do not overlap in resting muscle.

## 2.2 Mechanism of Muscle Contraction

Muscle contraction is a combination of electrical and mechanical events in a muscle fiber and start at the neuromuscular junction. The basic unit of contraction is a **motor unit**, composed of a group of muscle fibers and the somatic motor neuron that controls them. When the somatic motor neuron fires an action potential, all muscle fibers in the motor unit contract. The major steps leading up to skeletal muscle contraction can be summarized as follows:

1. Events at the neuromuscular junction convert a chemical signal from a somatic neuron into an electrical signal in the muscle fiber.
2. Muscle action potentials initiate calcium ( $\text{Ca}^{+2}$ ) signals which then activate the contraction-relaxation cycle.
3. The contraction-relaxation cycle can be explained by the sliding filament theory of contraction.

### 1. The contraction process begins at the neuromuscular junction

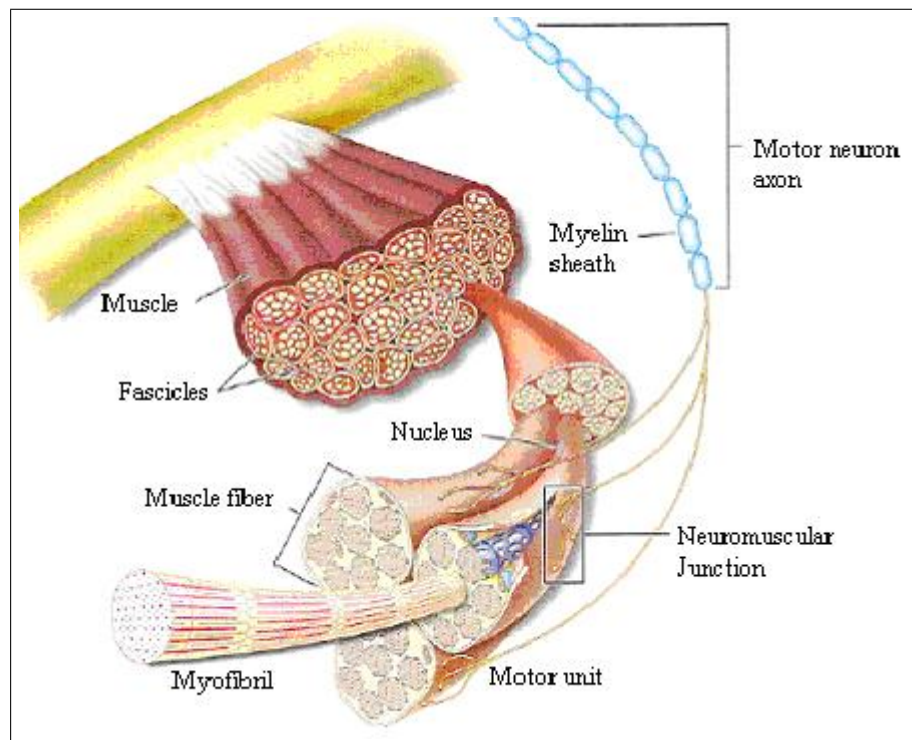


**Figure 2.4** Neuromuscular junction and a single alpha-motor unit [5].

The electrical discharge at the muscle initiates chemical events at the cell surface, releasing intracellular  $\text{Ca}^{+2}$  and ultimately causing muscle action. The nerve impulse (action potential) causes the release of acetylcholine (ACh) from the synaptic cleft. The binding of ACh to the receptors on the sarcolemma initiates a wave of depolarization. The action potential also propagates along the membrane lining the transverse tubules entering the cell. This action potential traveling along the T tubules causes the sarcoplasmic reticulum to release calcium into sarcoplasm.

**2. Muscle fiber stimulation causes an increase in intracellular  $\text{Ca}^{+2}$ , which precedes contractile activity.**

Intracellular  $\text{Ca}^{+2}$  plays an intimate role in regulating a muscle fiber's contractile and metabolic activity.  $\text{Ca}^{+2}$  concentration within a nonactive muscle fiber remains relatively low when compared with that of the extracellular fluid. Cellular  $\text{Ca}^{+2}$  increases when the action potential at the transverse tubules causes  $\text{Ca}^{+2}$  release from the sarcoplasmic reticulum. The inhibitory action of troponin (which prevents actin-

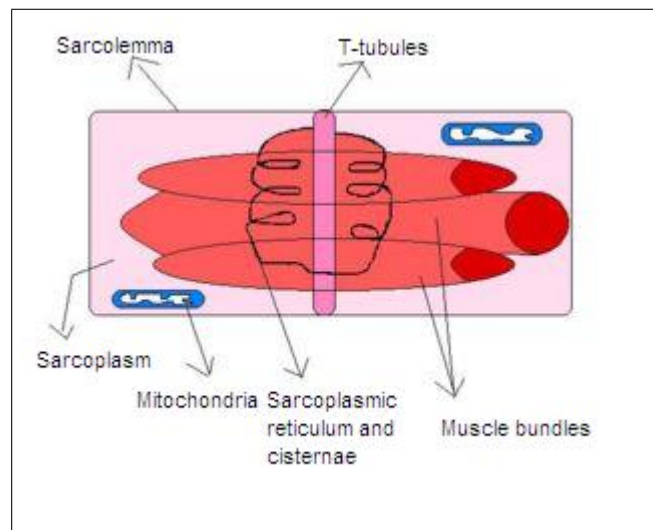


**Figure 2.5** The schematic diagram of skeletal muscle contraction.

myosin interaction) rapidly dissipates when  $\text{Ca}^{+2}$  binds with this and other proteins in the actin filaments [5].

Each myosin molecule is actually an ATPase and has two binding sites on it: one for an ATP molecule and one for actin. The actin molecules resemble a rope to which myosin heads bind. **Troponin** is a  $\text{Ca}^{+2}$  binding protein that controls the position of **tropomyosin**. Tropomyosin is actually an elongated polymer that wraps around the actin filament and blocks the myosin-binding sites. When  $\text{Ca}^{+2}$  binds with troponin, troponin changes the orientation of tropomyosin and that, in turn; exposes myosin-binding sites on actin. As  $\text{Ca}^{+2}$  ions join the active sites on actin and myosin, myosin ATPase is activated and hydrolyses ATP to ADP and inorganic phosphate ( $\text{P}_i$ ).

The energy generated causes myosin crossbridge movement to produce muscle tension. The crossbridge uncouples from actin when ATP binds to the myosin crossbridge. Coupling and uncoupling continues as long as  $\text{Ca}^{+2}$  concentration remains high enough to inhibit the troponin-tropomyosin system. This process is called excitation-contraction coupling. Figure 2.8 illustrates the interaction between actin and myosin.

In the relaxed state, troponin and tropomyosin interact with actin and this interaction prevents the myosin crossbridge from coupling to actin. During muscle

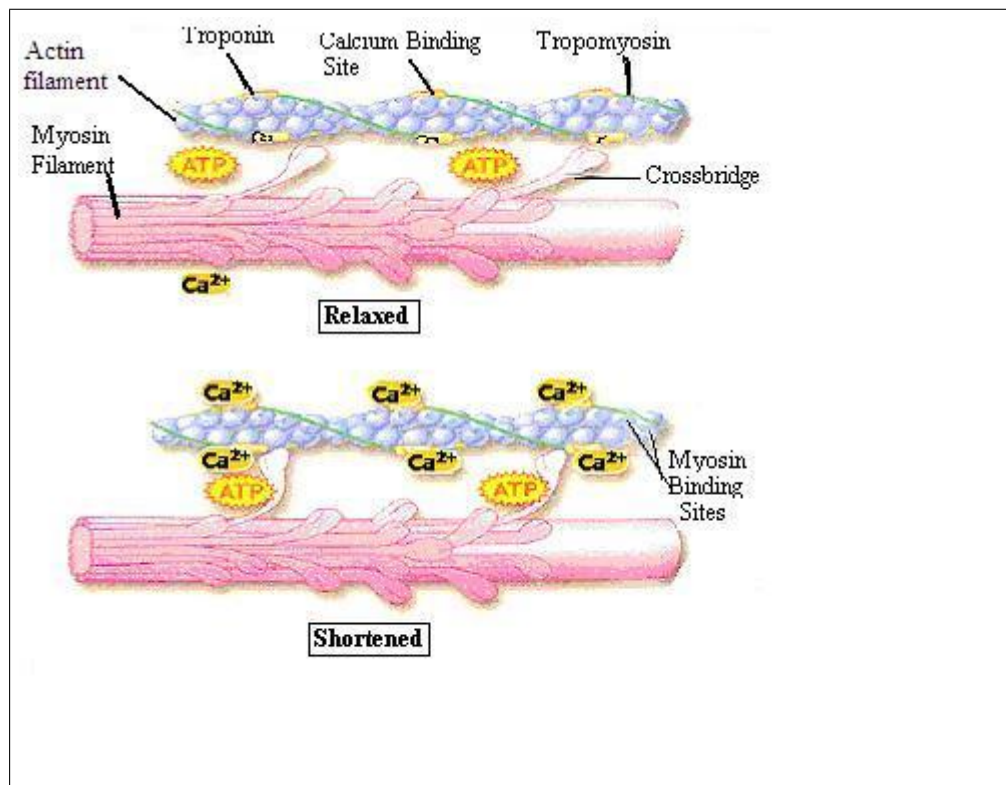


**Figure 2.6** Interaction between actin, myosin,  $\text{Ca}^{+2}$  and ATP in relaxed and shortened muscle [6].

action, the crossbridge couples with actin because of  $\text{Ca}^{+2}$  binding with troponin-tropomyosin

Figure 2.9 represents the structural arrangement of actin and myosin filaments during rest and contraction. Thick filaments pull on the actins toward the center by use of cross bridges. The sliding movement shortens the length of the entire sarcomere resulting from the attachment of actin filaments to the Z-line.

**3. The contraction-relaxation cycle can be explained by the sliding filament theory of contraction at the molecular level.**

1- **The rigor state.** Myosin heads are tightly bound to a G-actin molecule. In this state, no nucleotide (ATP or ADP) occupies the second binding site on the myosin head.

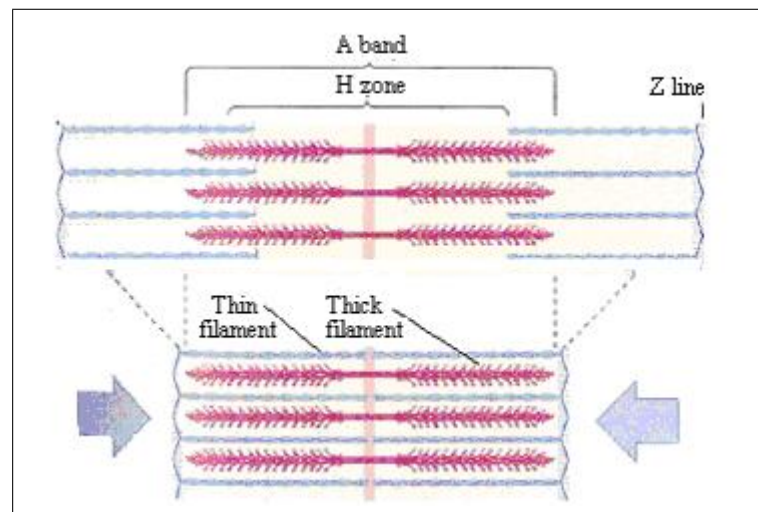


**Figure 2.7** Structural arrangement of actin and myosin filaments at rest and during contraction [6].

2- **ATP binds and myosin detaches.** An ATP molecule binds to the myosin head. This changes the actin-binding affinity of myosin and the myosin head releases from actin.

3- **ATP hydrolysis.** The binding site on myosin closes around ATP and hydrolyses it to ADP and inorganic phosphate ( $P_i$ ). Both of them remains bounded to myosin.

4- **Myosin reattachment.** The energy released from ATP rotates the myosin molecule, which binds weakly to a new G-actin molecule, one or two positions away from the G-actin to which it was previously bound. At this stage, myosin has potential energy, like a stretched spring, and is ready to execute the power stroke that will move the actin filament past it. ADP and  $P_i$  are still bound to myosin.

5-  **$P_i$  releases and the power stroke.** The power stroke begins when  $P_i$  is released from myosin binding site. As myosin rotates, it pushes the attached actin filament toward the center of sarcomere.

### 2.3 Length Dependence of Force Production in Skeletal Muscle

The force-length relationship of sarcomeres may be explained by the sliding filament and the cross-bridge theories. The sliding filament theory assumes that length changes in sarcomeres, fibers, and muscles are accomplished by relative sliding of the myofilaments, actin and myosin, within a sarcomere. Length of the A band remains constant despite the shortening of the sarcomere. The changes in length are consistent with the sliding of thin actin filaments along the thick myosin filaments as the actin filaments move toward the M line in the center of the sarcomere [7]. The cross-bridge theory suggests that the relative sliding of actin and myosin is caused by independent force generators which are namely the cross bridges [8].

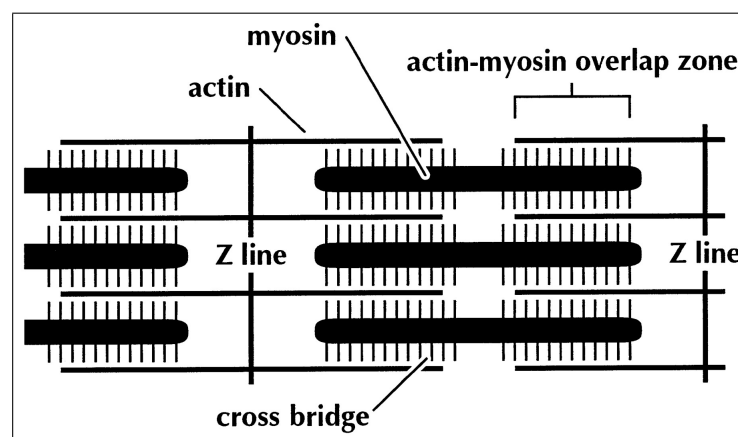


**Figure 2.8** Schematic representation of a sarcomere [1].

Cross bridges have a limited attachment range and the attachments occur only in the actin-myosin overlap zone of a sarcomere. This limitation implies that the maximal isometric force of a sarcomere is linearly related to the amount of actin-myosin overlap.

The force-length relationship of a striated muscle exhibits a characteristic curve in which the plateau and descending limb can be explained in terms of filament overlap [7]. On the ascending limb of the force-length relationship, active isometric sarcomere force decreases with decreasing length. Two conceptual possibilities are proposed for such a decrease in force in this region of the force-length relationship: 1) active force production may be reduced or 2) internal forces may oppose the active forces. It

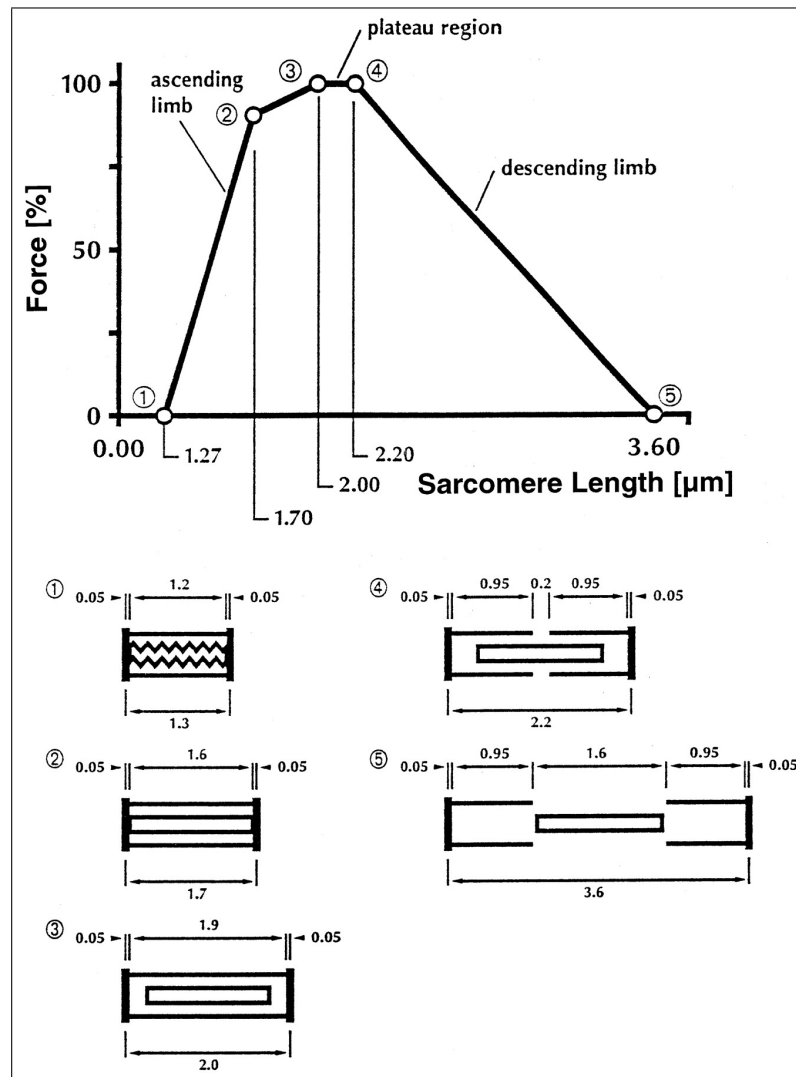


**Figure 2.9** Force-length relationship of frog skeletal muscle sarcomere, as derived first by Gordon et al. (top), and schematic sarcomeres corresponding to points (1-5) labeled on the force-length curve (bottom) [7].



has been suggested that force generation is inhibited by structural alterations such as double overlapping thin filaments and the collision of the ends of thick filaments with Z lines.

Active force is defined as the rise in force observed on activation of a muscle and is associated with cross-bridge interactions between myosin and actin [1]. Active force production may be reduced because of an increasing lateral distance between the actin and myosin filaments at short length effecting reduced probability of cross-bridge interaction [9]. Interference of cross-bridge interaction may occur with double overlap of the thin filaments. Also, below sarcomere lengths of  $1.7 \mu\text{m}$  (Figure 2.9), proper cross-bridge attachments may be limited due to deformation of the myosin filament [7].

Internal forces that may oppose active forces include forces associated with deforming actin and myosin filaments. Myosin deformation occurs when the Z lines of the sarcomere push against the ends of the myosin filament and appears to cause a decrease in force [7]. Furthermore, fluid and osmotic pressures may be elevated in shortened muscle fibers and may contribute to oppose the active sarcomere forces, as suggested by Sato et. al. and Gordon et al. [10, 7].

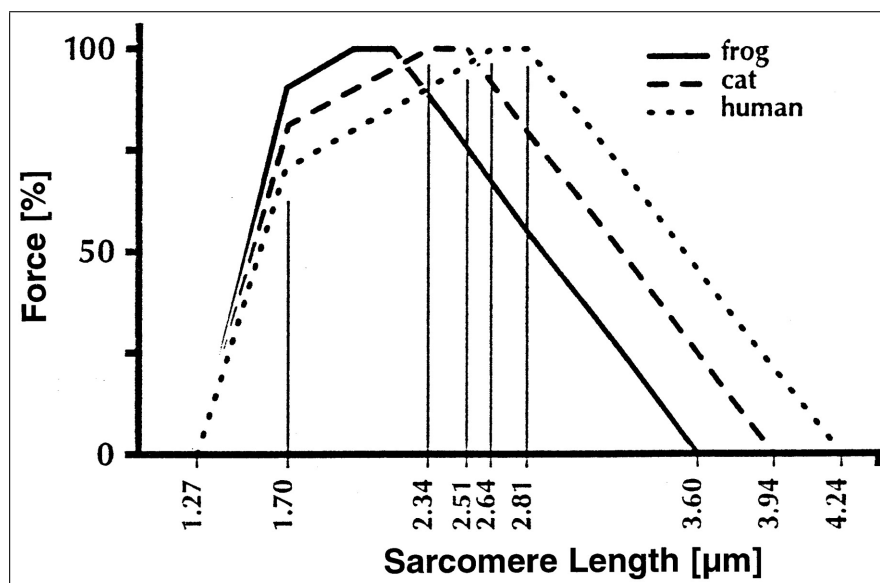


**Figure 2.10** Sarcomere force-length relationship in frog, cat, and human skeletal muscles [1].

Actin filament lengths vary appreciably across species, and this variation may

influence the shape of the sarcomere force-length relationship [11]. For example, the theoretical plateau region and descending limb of cat and human skeletal muscles are shifted to the right of that for frog. The ascending limb region for human and cat sarcomeres has not been determined.

## 2.4 Myofascial Force Transmission

In most classical muscle biomechanic experiments, it is assumed that the force exerted by skeletal muscle to generate motion is transmitted exclusively via the myotendinous junction. However, recent studies have shown that force is transmitted also through the inter- and extramuscular connective tissues. Myofascial force transmission is transmission of force from the full perimeter surface of myofibrils onto the extracellular matrix [4].

Transmission of force between myofibers is called intramuscular myofascial force transmission. Force transmission from muscle to surrounding non-muscular elements such as blood vessels, nerves, septum, membrane, and bone is called extramuscular myofascial force transmission. Also force is transmitted from extracellular matrix of a muscle to extracellular matrix of neighbor muscle. This is called intermuscular myofascial force transmission. This type of force transmission can be (1) from direct connections between muscles, and (2) from extramuscular myofascial connections. Inter- and extramuscular connections have continuous structure and they are defined as epimuscular myofascial connections [12].

## 2.5 Energy Metabolism in Skeletal Muscle

Muscles require energy constantly: (i) during contraction for cross bridge movement and release, (ii) during relaxation to pump  $\text{Ca}^{+2}$  back into sarcoplasmic reticulum, and (iii) after excitation-contraction coupling to restore  $\text{Na}^{+}$  and  $\text{K}^{+}$  to the extra

cellular and intracellular compartments, respectively.

Muscles contain phosphocreatine (PCr) as a back-up energy source. Phosphocreatine is a molecule in which high-energy phosphate bonds are created from creatine (Cr) and ATP when muscles are at rest. As the muscle is activated, such as during exercise, the high-energy phosphate group of PCr is transferred to ADP, creating more ATP to power the muscles.

Energy stored in high-energy phosphate bonds is very limited, so muscle fibers must use alternate metabolic pathways to transfer energy from the chemical bonds of nutrients to ATP. Carbohydrates, particularly glucose, are the most rapid and efficient source of energy for ATP production. Glucose is metabolized through glycolysis to pyruvate. In the presence of adequate  $O_2$ , pyruvate goes into the citric acid cycle, producing about 30 ATP for each molecule of glucose. There are 3 different muscle metabolic systems that supply the energy required for various activities :

- Phosphagen system (for 10-15 second bursts of energy)
- Glycogen lactic acid system (for another 30-40 seconds of energy)
- Aerobic system (provides the greatest deal of energy)

The aerobic system in the body is used for activities that require an extensive expenditure of energy. A large amount of ATP must be provided to muscles in order to sustain the muscle power needed to perform such activities. This can only be accomplished when  $O_2$  in the body is used to break down the pyruvic acid (that was produced anaerobically) into carbon dioxide, water, and energy by a complex series of reactions known as the **citric acid (Krebs)** cycle. The breakdown of pyruvic acid requires oxygen and slows or eliminates the accumulation of lactic acid [5].

The most efficient production of ATP occurs through aerobic pathways such as the glycolysis-citric acid cycle pathway. If the cell has adequate amounts of oxygen

for oxidative phosphorylation, then both glucose and fatty acids can be metabolized to provide ATP. As the oxygen requirement of a muscle fiber exceeds its oxygen supply, energy production from fatty acids decreases dramatically and glucose metabolism shifts to anaerobic pathways. Anaerobic metabolism is also known as glycolytic metabolism, because in low oxygen conditions, anaerobic glycolysis is the primary pathway for ATP production. When a cell lacks oxygen for oxidative phosphorylation, the final product of glycolysis, pyruvate, is converted to lactic acid [5].

Anaerobic metabolism has the advantage of speed, producing ATP 2.5 times as rapidly as aerobic pathways do. However, anaerobic metabolism provides only two ATP per glucose, compared with the average of 30-32 ATP per glucose for oxidative metabolism, and it contributes to a state of metabolic acidosis by producing lactic acid [5].

## **2.6 Blood Flow and Oxygenation of Skeletal Muscle**

Arteries and veins are oriented parallel to individual muscle fibers, and provide muscles with a rich vascular supply. These vessels are further branched into capillaries, arterioles and venules forming a network in and around the endomysium. Extensive branching of blood vessels, in and around the endomysium, assures each muscle fiber of an adequate supply of oxygenated blood from the arterial system and rapid removal of carbon dioxide in the venous circulation. Blood flow is redistributed as a result of a combination of vasodilation -which decreases peripheral resistance to blood flow- in skeletal muscle and vasoconstriction in other tissues in order to accommodate the oxygen requirement during exercise [6].

As exercise commences,  $O_2$  consumption increases rapidly. However, this increase is not matched immediately by the oxygen supply to the muscles. During the lag time, ATP is provided by muscle ATP reserves, PCr, and aerobic metabolism supported by oxygen stored on muscle myoglobin and blood hemoglobin [6, 5].

The use of these muscle stores creates an oxygen deficit because their replacement requires aerobic metabolism and  $O_2$  uptake. When exercise stops,  $O_2$  consumption slows down to resume its resting level. The excess post-exercise oxygen consumption (EPOC), represents oxygen being used to metabolize lactate, restore ATP and phosphocreatine levels, and replenish the  $O_2$  bound to myoglobin [5].

### 3. NEAR INFRARED SPECTROSCOPY

The use of optical methods exploiting near-infrared (NIR) radiation has been widely investigated for diagnostic purposes since Jöbsis first demonstrated that transmittance measurements of near-infrared (NIR) radiation could be used to monitor the degree of oxygenation of certain metabolites [13]. Starting with this pioneering work, near-infrared spectroscopy (NIRS) has found many applications in exercise physiology and neuroscience.

NIRS is a non-invasive and relatively low cost optical technique from which information can be obtained about the oxygenation of a biological tissue such as muscle tissue. Oxidative metabolism is the dominant source of energy for skeletal muscle. Therefore, noninvasive monitoring of oxygenation in exercising skeletal muscles and following their modification in response to specific training has been of great interest [14].

Recently, NIRS has become a widely used technique for measuring muscle  $O_2$  saturation and changes in haemoglobin volume. Although there are a number of methods to gather information about muscle energetics, NIRS offers the advantage of being easily applicable with regard to muscle performance and more comfortable and suitable for monitoring multiple muscle groups with higher resolution. Muscle  $O_2$  saturation represents a dynamic balance between  $O_2$  supply and  $O_2$  consumption in the small vessels such as arterioles and capillaries [15]. NIRS has been used to investigate diseases associated with impaired tissue oxygenation as well as human muscle performance in combination with other techniques such as surface electromyography (sEMG) and phosphorous magnetic resonance spectroscopy ( $^{31}P$ -MRS) [16].

The clinical significance of NIRS muscle findings in different diseases has been explored by several groups. NIRS has been used to investigate diseases associated with impaired tissue oxygenation, like heart failure and peripheral vascular disease (PVD).

It has been proven that patients with congestive heart failure desaturate their muscle at lower work levels than normal subjects indicating an insufficient blood flow to the exercising muscles of these patients [17, 18].

### 3.1 Theoretical Basis of NIRS

The physical principles of NIRS have been reported previously in detail by various investigators [14, 19]. NIR light (700-1000nm) penetrates skin, subcutaneous fat or skull and is either absorbed or scattered within the tissue. The absorption depends on the amount of oxygen that is present in the tissue. By measuring the absorption changes in at least two wavelengths in the near-infrared range, it is possible to find concentration changes of deoxygenated (Hb) and oxygenated hemoglobin (HbO<sub>2</sub>) with NIRS. The concentration changes are not absolute values but are determined relative to a baseline measurement. Thus; NIRS doesnot give information about absolute concentration values but rather gives dynamic balance information between O<sub>2</sub> supply and consumption. NIRS offers to be a non-invasive and inexpensive method for the study of aerobic metabolism and hemodynamics and has become a widely used technology for the oxidative metabolism investigation in tissues, especially in brain and muscle [20].

Continuous wave NIRS (NIR<sub>cws</sub>) technology is based on the fact that light in the wavelength range of 650-950 nm is weakly absorbed by tissues. When the light is transmitted through the tissue, part of it is absorbed and part of it is scattered. Human tissues contain a variety of substances whose absorption spectra at NIR wavelengths are well defined, and which are present in sufficient quantities to contribute significant attenuation to measurements of transmitted light. Biological tissue is relatively transparent for light in the near-infrared region of the electromagnetic spectrum. Light in the wavelength range below 650 nm is strongly absorbed by Hb whereas water is the dominant absorbing substance above 1000nm. However, within the 650-1000 nm wavelength range, it is possible with sensitive instrumentation to detect light which has traveled up to 8 cm of tissue [19]. This wavelength range is called the optical window.

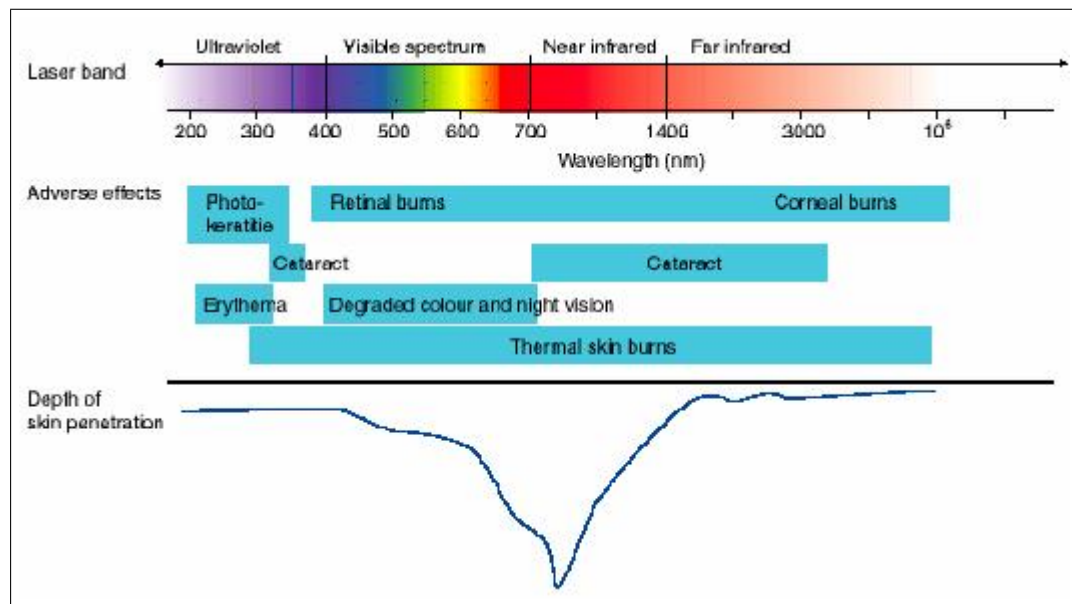


**Figure 3.1** Wavelength dependence of light absorption in terms of skin penetration [21].

The optical window is closely related to the range where the minimal absorption for water takes place due to the high content of water in all biological tissues. Whole blood is a strong absorber in the red-near infrared regime but the volume fraction of blood is a few percent in tissues, hence the average absorption coefficient that affects light transport is moderate. However, when photons strike a blood vessel, they encounter the full strong absorption of whole blood. Light passing through the large vessels is mostly absorbed thus, light that reaches the detector comes mainly from small blood vessels (arterioles, capillaries and venules) providing a better circumstance for measurement in extremities [20, 15].

### 3.2 Application of NIRS in Exercise Physiology

The majority of exercise studies using NIRS have been descriptive to ascertain that this technique can be used to examine alterations in muscle deoxygenation and blood volume during short-term acute exercise [23]. NIRS has found a number of applications in the study of haemodynamic and oxygenation-related parameters in tissue and exercise induced changes in muscle metabolism.



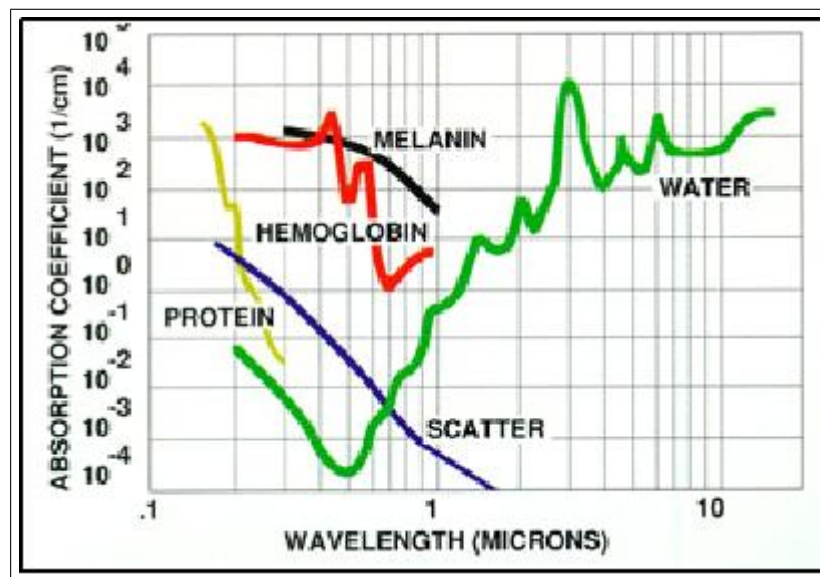


**Figure 3.2** Absorption coefficients of various biological tissue components (adapted from BM585 lecture notes) [22].

NIRS can objectively evaluate muscle oxidative metabolism in athletes and its modifications following potential therapeutic strategies and specific training programs. Various approaches utilizing NIRS for enhancement of muscular and neural performance have been applied recently. Mancini et al. have shown NIRS to be a valid [17] and reliable technique for measuring relative changes in muscle deoxygenation and blood volume. It has been demonstrated that the rate of  $O_2$  resaturation after exercise is faster in the endurance trained athlete (rowers) than in sedentary controls in a study performed by Chance et al [24].

Different NIRS approaches have been applied for studying muscle pathophysiology and exploring oxidative metabolic responses of working and non-working muscle groups to different sport activities. The first application of NIRS in sports goes back to 1992 when Chance et al. investigated the recovery from exercise-induced deoxygenation in the quadriceps muscles of elite competitive rowers. They demonstrated that the re-oxygenation times provide a non-invasive localized indication of the degree of oxygen delivery stress in the exercised limb. Later, following muscle metabolic response to field activities became possible thanks to the development of more ac-

curate portable NIR<sub>cws</sub> devices. Quaresima et al. investigated vastus lateralis and rectus femoris VO<sub>2</sub> at rest and during MVC using a 12-channel NIR<sub>cws</sub> system [25]. mVO<sub>2</sub> value was significantly higher than that of at rest. The results indicated that NIRS can be used for investigating the spatial and temporal features of muscle oxygenation.

The monitoring of a single muscle fiber location does not accurately represent the heterogenous oxidative metabolic responses to the same exercise either within the same muscle or among different muscle groups. The ongoing development of multi-channel NIRS devices offer promising solutions to this problem. In the last decade, multi-channel NIR<sub>cws</sub> systems have been developed to provide spatial maps of oxygenation changes every 5-8 sec. Miura et al., found regional differences in the oxygenation of the gastrocnemius during plantar flexion exercise and recovery with the distal portion having greater oxygenation. This is a reasonable result since distal portion has a greater change in BF possibly because of the higher intramuscular pressure during exercise [26].

In the eighties, several NIR<sub>cws</sub> prototypes were built [13, 27, 19, 24]; forearm occlusion and exercise was used to test their instrumental capabilities [14]. Hampson and Piantadosi first investigated the changes in forearm muscles oxygenation during tourniquet ischaemia and venous outflow restriction [27]. Cheatle et al. demonstrated that mVO<sub>2</sub> can be measured in the calf by calculating the rate of conversion of oxyhaemoglobin to deoxyhaemoglobin during a period of tourniquet-induced ischaemia [28]. This method was also used by De Blasi et al. at rest and during forearm exercise achieved with and without vascular occlusion. The MVC, performed during vascular occlusion, caused a complete desaturation in 10-15 sec, which was not followed by any further desaturation when the second contraction was performed. No difference was found in mVO<sub>2</sub> measured during MVC with and without vascular occlusion [20]. Collier et al. studied the relationship between mVO<sub>2</sub> in the soleus muscle and the level of isometric exercise expressed as percentages of MVC. A linear relationship was found between the mVO<sub>2</sub> and the level of exercise [2].

The validity of the mVO<sub>2</sub> method was examined by several investigators. In

a study by Sako et al., results from  $^{31}\text{P}$ -MRS measurements were used as a standard for NIRS measurements. Subjects performed two sets of handgrip exercise, once for the NIRS measurement and once for the  $^{31}\text{P}$ -MRS measurement as a standard. There was a significant correlation between the  $\text{mVO}_2$  values measured by the two methods. In another study by Hamaoka et. al , again  $^{31}\text{P}$ -MRS and NIRS were used together to evaluate muscle oxygen consumption [29]. The initial rate of finger flexor de-oxygenation during immediate postexercise muscle ischaemia was found to be a reflection of muscle  $\text{mVO}_2$  [30].

Van Beekvelt et al. investigated  $\text{mVO}_2$  and blood flow in resting and exercising forearm during sustained isometric handgrip exercise by NIRS and compared the results with global muscle  $\text{mVO}_2$  data and forearm blood flow derived from the Fick method and plethysmography [31]. This study concluded that NIRS is an appropriate tool to provide information about local  $\text{mVO}_2$  and local forearm blood flow because both place and depth of the NIRS measurements reveal local differences that are not detectable by the Fick method. These methods were also successfully used by Homma et al. who estimated forearm blood flow and muscle oxygen consumption during venous occlusion imposed at rest and immediately after handgrip exercise with loads equal to 5 %, 10 %, 15 %, 20 %, 25 %, and 30 % of the MVC [32].

In an attempt to investigate the effects of cardiac fatigue on  $\text{O}_2$  dynamics, Kasıkcıoğlu et. al. designed a study to evaluate the changes of left ventricular function, exercise capacity and skeletal muscular oxygen kinetics after fatiguing exercise. The subjects were examined firstly by echocardiography, secondly by cardiopulmonary exercise testing and then by NIRS, before and after marathon competition. A decrease in left ventricular systolic and diastolic functions was accompanied by an increase in half time of muscular oxygen delivery after race period. The results indicate that NIRS measurements of  $\text{O}_2$  kinetics can be used in conjunction with cardiopulmonary exercise testing for detecting cardiac fatigue [33].

To sum up, the existing studies indicate that NIRS is a potential tool for being applied successfully in sports medicine. Human muscle performance and oxygen con-

sumption evaluation techniques (fMRI, blood oxygenation level dependent (BOLD) contrast MRI, P-NMRS and  $^{31}\text{P}$  MRS) are being utilized to increase our knowledge about the muscle performance and metabolic processes . However, these techniques are expensive, physically constraining, and confine the participants to restricted positions. The disadvantages give preference to fNIRS due to (i) ease in measurement, (ii) noninvasive use, (iii) application at the tissue level, (iv) ability to give information about tissue oxyhemoglobin and deoxyhemoglobin concentration changes during short periods of ischemiacite [34]. NIRS is a portable, relatively inexpensive, and negligibly invasive modality, and can be used repeatedly with the same participants. It is likely that NIRS will keep on presenting itself as an objective quantization methodology for oxidative metabolism in athletes and its modifications following potential therapeutic strategies and specific training programs.

## 4. METHOD

### 4.1 Subjects

Nine voluntary healthy male subjects participated in the study. All subjects were briefly informed about the experimental protocol and informed consent was obtained before the test. The subjects came to our laboratory on four different days.

### 4.2 Experimental Protocol

Subjects sat in a backward-inclined ( $15^\circ$ ) chair that allows the upper arm to extend to the level of the heart, with the right hand resting on a hand dynamometer. The arm rested on a platform with an elbow angle close to 120 degrees. NIRS measurements were carried out on top of flexor digitorum superficialis (FDS) muscle. The NIRS probe was placed on the medial part of the anterior compartment of right forearm. The measurement site was centered around the most active site during handgrip exercise which actually corresponds to the superficial layers of FDS.

Subjects were asked to perform a sustained handgrip exercise by continuously pressing on a handgrip dynamometer. The handgrip exercise was performed at 3 different wrist positions: (i) wrist in neutral position, (ii) wrist maximally flexed and (iii) wrist maximally extended. At each wrist position, 4 separate sessions took place at varying force levels (10 %MVC, 20 %MVC, 30 %MVC, 40 %MVC). The subject's maximum voluntary contraction force (MVC) were determined prior to each exercise. The intensity of each exercise session was based on the individual maximum force production as determined prior to the test.

The tests were performed on 4 different days and the probe position was marked on the arm by waterproof markers in order to avoid variation in placement over separate

days. The order of experiments were randomized.

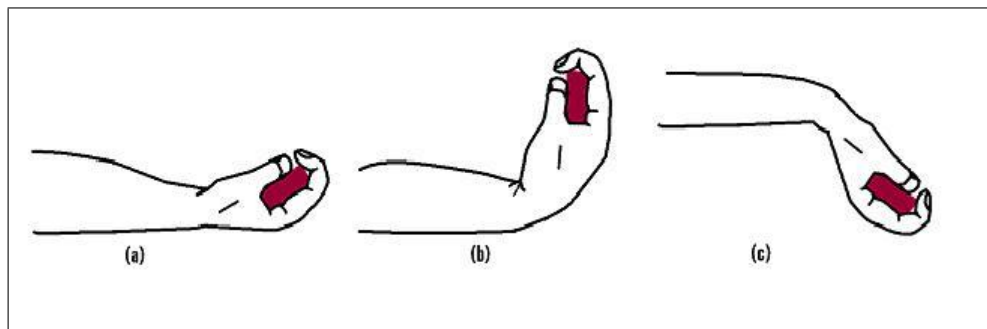


**Figure 4.1** The handgrip exercise was performed at 3 different wrist positions (top view). a) wrist in neutral position b) wrist maximally flexed c) wrist maximally extended.

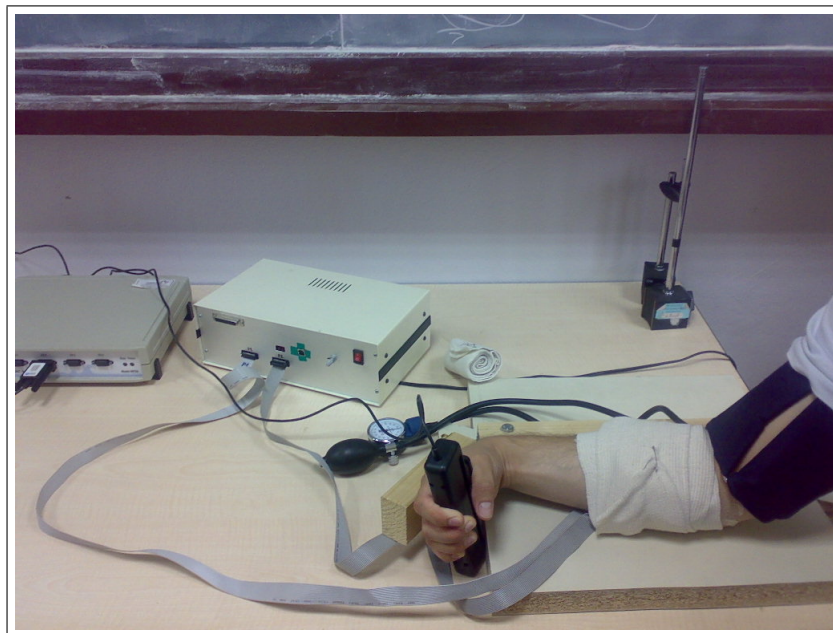


**Figure 4.2** The handgrip exercise while the wrist is maximally flexed.

After placing the probe on the right arm properly, the experiment began with a 30 seconds of rest period followed by an arterial occlusion. A pneumatic cuff placed around the upper arm was used to apply arterial occlusion at a pressure of 220 mmHg during the test. Ten seconds of delay period was required for monitoring basal metabolic response to cuff ischaemia. After ten seconds of delay, the subject started

to grip the hand dynamometer continuously at the predetermined force level and wrist position. Each session took approximately 10 minutes, consisting of four different periods:

- 30 seconds of introductory period (IP) followed by cuff inflation.
- Basal metabolism measurements during arterial occlusion.
- Exercise period with arterial occlusion (AO).
- Recovery period (R).

### 4.3 Data Collection

The instrument that was used for quantification of the results obtained by NIRS was developed at Boğaziçi University, Biophotonics Lab [35]. The device houses a probe that contains a light emitting diode (LED) and 4 photodetectors arranged in the form of a linear array. The light source and detectors are embedded on a flexible printed circuit board (PCB). The light source is a multiwavelength LED and emits light at three near infrared wavelengths; 730nm, 805nm and 850nm. The photodetectors are placed 1cm apart and the source detector distance varies from 1 cm to 4 cm.

The emitted light travels through the skin, subcutaneous fat or tissue and is either absorbed or scattered from the tissue. The portion of light that returns to the detectors is mostly collected from a penetration depth of one half the source-detector distance[15]. Light from the emitter at 735 nm is more easily absorbed by Hb, while light at 850 nm is more easily taken up by HbO<sub>2</sub>. The intensity of light that returns to the detectors can be measured and converted into concentration changes of Hb and HbO<sub>2</sub> by use of a modification in the Lambert-Beer Law.

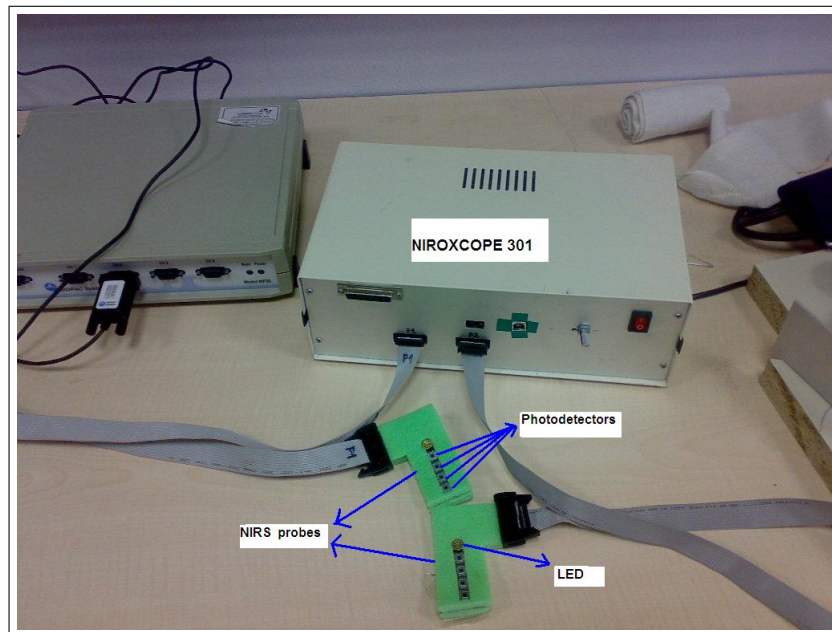


**Figure 4.3** Components of NIROSCOPE 301.

## 4.4 Data Analysis

NIROSCOPE 301 provides plots of concentration changes of  $[Hb]$  and  $[HbO_2]$  of the tissue being probed in a case of blood volume constancy. The program developed in the MATLAB environment is utilized for calculating local oxygen consumption ( $mVO_2$ ) during exercise and post exercise recovery time ( $t_{rec}$ ).

Figure 4.4 illustrates a typical example of the NIRS signals during a single exercise intensity at 10 % MVC.

During the exercise period, blood volume is kept constant by applying cuff ischaemia. The concentration changes of  $[Hb]$  and  $[HbO_2]$  move in opposite directions (except for the initial part where total ischemia had not been established yet). As there is not a blood supply to the region,  $[Hb]$  continuously increases until it reaches a steady state.  $[HbO_2]$  may take an initial positive value due to rushing of the blood into the forearm from the pumping action of the cuff as soon as arterial occlusion



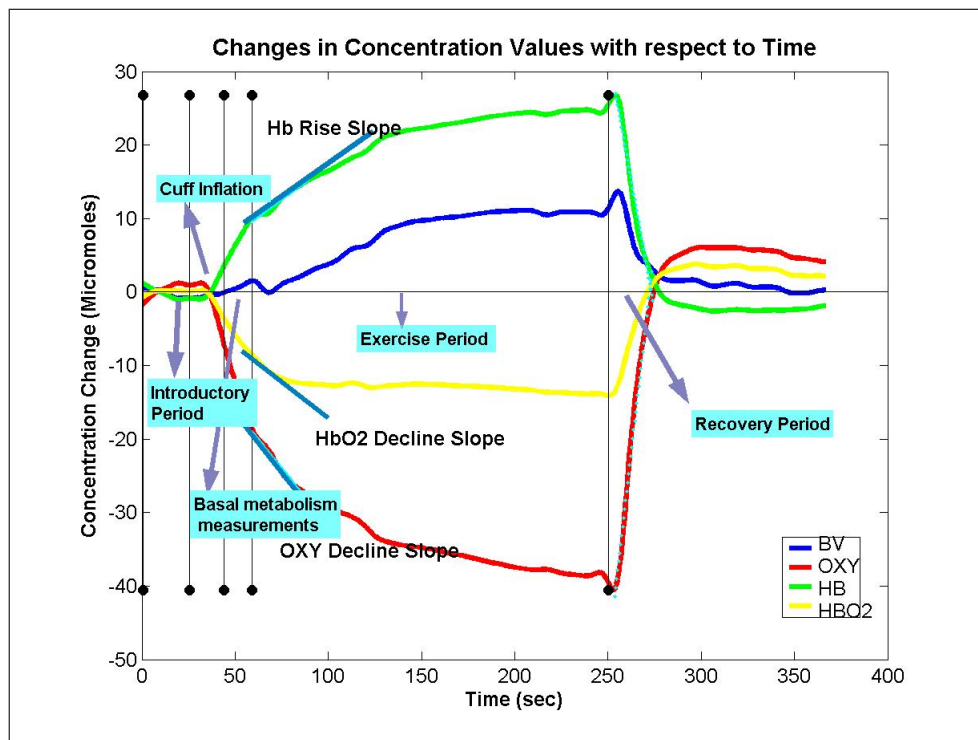


**Figure 4.4** A typical example of the NIRS signals in an individual subject during a single exercise intensity at 10 % MVC.

occurs. Later, it decreases as oxygen in the region is continuously used up and HbO<sub>2</sub> is converted into Hb. All signals reach a steady state when the oxygen in the region is completely depleted. This steady state tends to appear faster as the exercise intensity increases.

In the recovery period, the effect of arterial occlusion is progressively recovered. As soon as ischemia is released, the accumulated Hb is replaced by HbO<sub>2</sub> due to the rushing blood from the newly-opened arteries. The restoration of blood causes a sharp fall in [Hb] and a sharp rise in [HbO<sub>2</sub>]. As time progresses, both signals establish an equilibrium, not necessarily at the original baseline level. This phenomenon suggests that ischemia is creating a permanent effect on the muscle if sufficient resting time is not provided. Hence; the exercise sessions that were to be carried out on the same day were separated by at least 2 hours.

#### 4.4.1 Interpretation of the Signals

After the release of the arterial occlusion, [Hb] decreases and reaches minimum point; meanwhile [HbO<sub>2</sub>] increases and reaches maximum point. The time between the release of the ischemia and the first time a signal reaches the initial 0 (zero) value is denoted as the recovery time ( $t_{rec}$ ) for that signal. From the [HbO<sub>2</sub>] and [Hb] signals, OXY signal is also evaluated which reflects difference between concentration changes of [HbO<sub>2</sub>] and [Hb] ( $\Delta[HbO_2]-\Delta[Hb]$ ). The time course of recovery of the 3 signals are analyzed as a measure of oxygen stress in the exercised limb.

The initial oxygen consumption rate during exercise is calculated by three methods: (i) from the rate of decrease in the OXY and (ii) [HbO<sub>2</sub>] signals after occlusion begins; and (iii) from the rate of increase in the [Hb] signal at the onset of exercise. The mVO<sub>2</sub> during exercise period with arterial occlusion can be calculated from the rate of decrease in [HbO<sub>2</sub>] [36, 30, 2, 37] or from the rate of decrease in the OXY signal [38, 36, 25]. Another evaluation method is to analyze the initial linear increase in the [Hb] signal which appears to be a mirror image of the [HbO<sub>2</sub>] signal [31]. All three methods reflect the rate of conversion of HbO<sub>2</sub> to Hb during a period of arterial occlusion-induced ischaemia.

The mVO<sub>2</sub> values were calculated while the signals had a linear change at the onset of exercise because in this period of linear change, the energy consumption would be dependent mainly on aerobic processes. Hence; the measured mVO<sub>2</sub> gave an indication of local energy consumption. The exact time window that was used for fitting a linear regression line to the concentration changes versus time curves varied over different work intensities.

#### 4.4.2 Statistical Data Analysis

For all parameters involved, the mean and the standard deviation values are calculated. Statistical significance between groups was tested by the 2-Way Analysis of

Variance Test (**anova2** in MATLAB 7.0). The statistically significant level of difference was considered to be at  $p < 0.05$ . **anova2** function in MATLAB performs a balanced two-way analysis of variance for comparing the means of two or more columns and two or more rows of the observations in a group of data. The data in different columns represent changes in one factor (muscle length in our case) whereas data in different rows represent changes in another factor (exercise intensity).

## 5. RESULTS and DISCUSSION

### 5.1 mVO<sub>2</sub> During Exercise

mVO<sub>2</sub> during exercise was measured from the rate of increase in the [Hb] signal during arterial occlusion. mVO<sub>2</sub> was also calculated from the rate of decrease of the [HbO<sub>2</sub>] and OXY signals during the arterial occlusion period but the results could not be proven to be statistically different. Table 5.1 shows the mVO<sub>2</sub> values calculated from the [Hb] signal.

**Table 5.1**

mVO<sub>2</sub> calculated from the changes in [Hb] signal with respect to time at the onset of exercise. Data are represented in units of micromoles per second ( $\mu\text{moles/s}$ ) and the findings are expressed as mean  $\pm$  standard deviation.

Exercise Level	mVO <sub>2</sub> (Hb)		
	Neutral	Maximal Flexion	Maximal extension
10%MVC	0.23 $\pm$ 0.18	0.27 $\pm$ 0.17	0.15 $\pm$ 0.11
20%MVC	0.26 $\pm$ 0.19	0.32 $\pm$ 0.11	0.19 $\pm$ 0.10
30%MVC	0.34 $\pm$ 0.17	0.42 $\pm$ 0.24	0.27 $\pm$ 0.18
40%MVC	0.43 $\pm$ 0.27	0.48 $\pm$ 0.21	0.38 $\pm$ 0.29
<b>p value</b>	<b>0.002</b>		

#### 5.1.1 The Relationship Between mVO<sub>2</sub> and the Level of Isometric Exercise

Figure 5.1 illustrates mVO<sub>2</sub> at increasing force levels for three wrist positions. An increase in mVO<sub>2</sub> with force level is observed (i) while the wrist is maximally flexed, (ii) while the wrist is in neutral position and (iii) while the wrist is maximally extended.

The relationship between mVO<sub>2</sub> and the level of isometric exercise can be evaluated by fitting a linear regression of the form

$$y(x) = ax + b \quad (5.1)$$

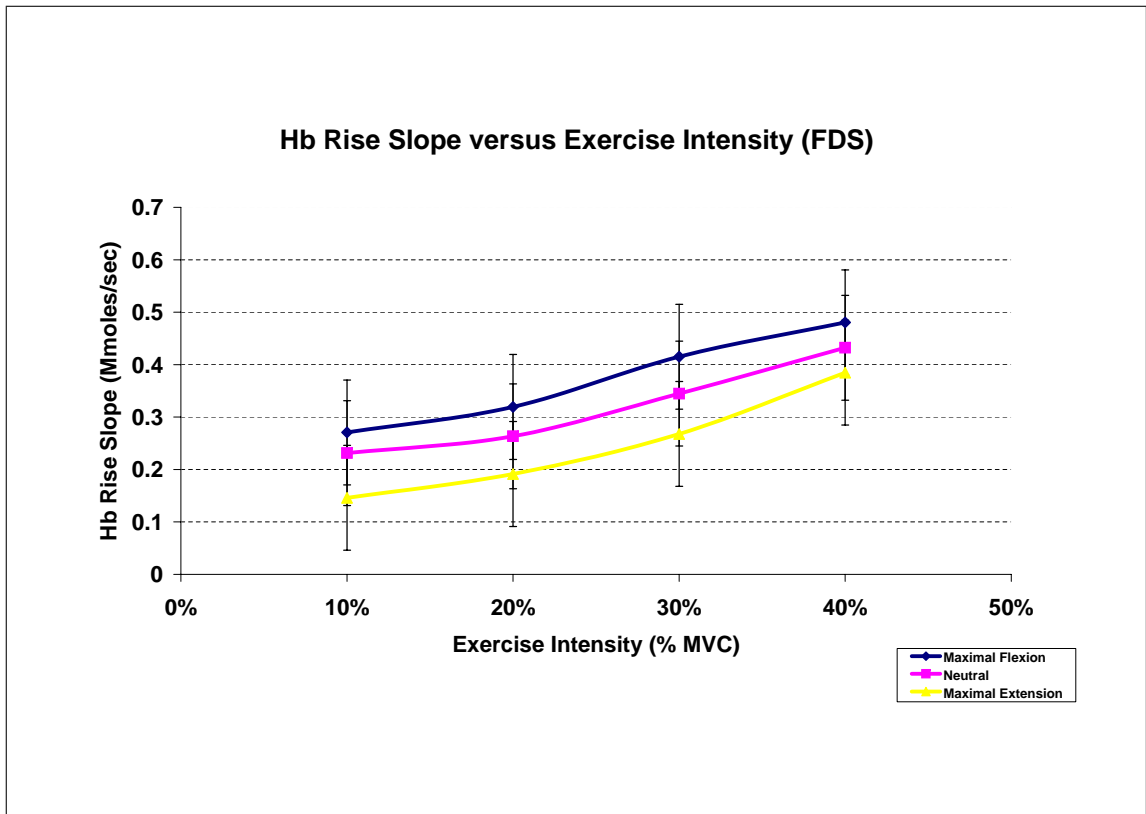


**Figure 5.1** Hb rise slope versus exercise intensity (data from Table 5.1).

where  $y(x)$  represents the [Hb] rise slope varying with exercise level (% MVC),  $a$  is the slope of the linear regression line ( $\mu\text{moles/s}$ ) and  $b$  is the intercept of the fitted line. The coefficients of the regression equations that are used to describe the relationship between  $m\text{VO}_2$  and the level of exercise at 3 wrist positions is given below:

**Table 5.2**  
Coefficients of regression equations and  $R^2$  values.

Wrist Position	$a$	$b$	$R^2$
Maximal Flexion	0.725	0.19	0.98
Neutral	0.689	0.147	0.96
Maximal Extension	0.792	0.05	0.96

### 5.1.2 The Effect of Wrist Position on the Relationship Between $m\dot{V}O_2$ and the Level of Isometric Exercise

Figure 5.2 illustrates  $m\dot{V}O_2$  at the onset of exercise at varying wrist positions. FDS muscle contributes to the flexion of the wrist [39]. Changing position of the wrist alters length of this muscle group to some extent which has not been quantified in vivo. Flexing the wrist maximally shortens while extending it maximally lengthens the FDS muscle.

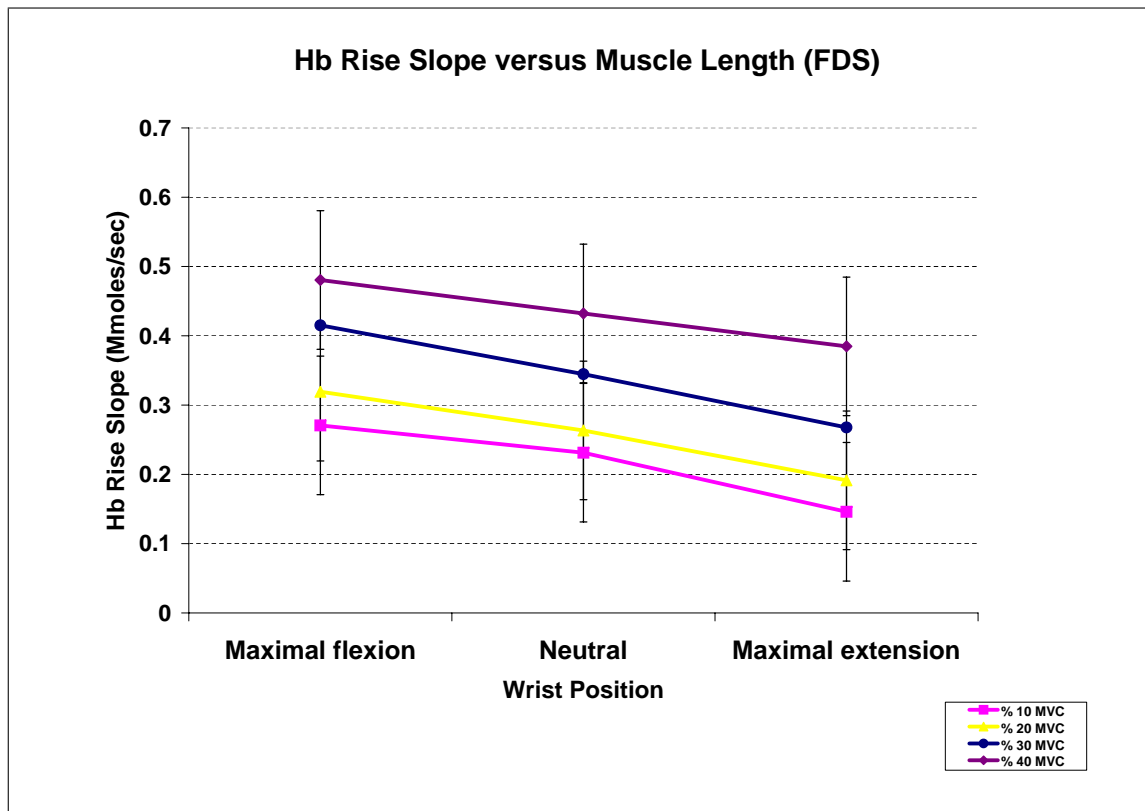


**Figure 5.2** Length dependent  $O_2$  consumption for FDS muscle (data from Table 5.1).

The slope of  $[Hb]$  rise during the initial period of exercise is averaged for 9 subjects for each exercise session. As the plot of  $[Hb]$  rise slope versus muscle length is examined, it is observed that

(i)  $mVO_2$  decreases with increasing length when the handgrip exercise is performed at the same exercise level. (ii)  $mVO_2$  increases with increasing contraction intensity (%MVC) and this result holds true for all 3 wrist positions.

## 5.2 Post-exercise Recovery Time ( $t_{rec}$ )

$t_{rec}$  reflects the balance between  $O_2$  delivery and  $O_2$  demand in a muscle after exercise, and it can be interpreted as the duration for repayment of  $O_2$  and energy deficiency accumulated during exercise by tissue respiration.  $t_{rec}$  is regarded as one of the indicators of muscle oxidative capacity because it is correlated with muscle  $O_2$  content and phosphorylation potential during exercise [24].

The time course of recovery of [Hb], [HbO<sub>2</sub>] and OXY signals were analyzed as a measure of oxygen stress in the exercised limb. Table 5.3 illustrates  $t_{rec}$  for the [Hb] signal.

**Table 5.3**

$t_{rec}$  measured from the Hb signal during exercise. Data are represented in seconds and the findings are expressed as mean  $\pm$  standard deviation.

Exercise Level	$t_{rec}$ (Hb)		
	Neutral	Maximal Flexion	Maximal extension
10%MVC	48.18 $\pm$ 19.26	24.88 $\pm$ 9.14	28.68 $\pm$ 9.77
20%MVC	62.65 $\pm$ 14.32	26.78 $\pm$ 6.03	30.27 $\pm$ 7.63
30%MVC	64.06 $\pm$ 22.92	29.58 $\pm$ 13.09	37.96 $\pm$ 9.26
40%MVC	84.58 $\pm$ 40.82	30.40 $\pm$ 9.16	57.63 $\pm$ 20.21
<b>p value</b>	<b>0.023</b>		

### 5.2.1 The Relationship Between $t_{rec}$ and the Level of Isometric Exercise.

Figure 5.3 illustrates  $t_{rec}$  for increasing force level for 3 wrist positions.  $t_{rec}$  increases with force level at all positions of the wrist. An increase in  $t_{rec}$  with increasing

exercise level is observed for all wrist positions.

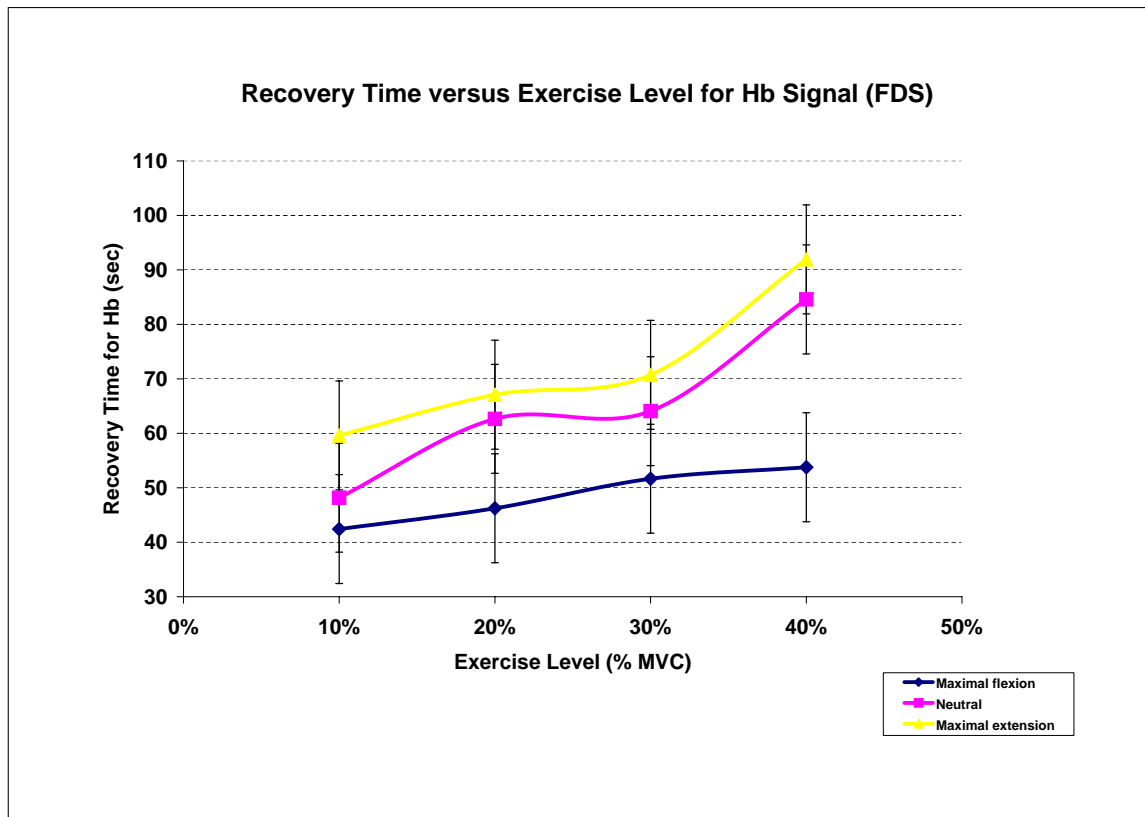


**Figure 5.3**  $t_{rec}$  versus exercise level for different positions of the wrist.  $t_{rec}$  increases with increasing force level at all wrist positions (Data from Table 5.3).

The relationship between  $t_{rec}$  and the level of isometric exercise is evaluated by fitting a linear regression line of the form

$$y(x) = ax + b \quad (5.2)$$

where  $y(x)$  represents  $t_{rec}$  for [Hb] signal varying with % MVC,  $a$  is the slope of the linear regression line and  $b$  is the intercept of the fitted line. The coefficients of the regression equations that are used to describe the relationship between  $t_{rec}$  and the level of exercise at varying lengths of FDS muscle are given below:

It can safely be claimed that  $t_{rec}$  increases linearly with contraction intensity for all positions of the wrist. The linearity is valid for all muscle lengths but no comment can be made on how alterations in length affect the slope of fitted linear lines.



**Table 5.4**  
Coefficients of regression equations and  $R^2$  values.

Wrist Position	a	b	$R^2$
Maximal Flexion	39.2	47.186	0.87
Neutral	110.62	37.21	0.9
Maximal Extension	39.47	38.65	0.97

### 5.2.2 The effect of altering wrist position on the relationship between $t_{rec}$ and the level of isometric exercise

Figure 5.4 illustrates  $t_{rec}$  for FDS muscle at varying wrist positions.  $t_{rec}$  obtained from [Hb] and OXY signals were proven to be statistically significant for FDS muscle. The results are averaged for 9 subjects for each exercise session.

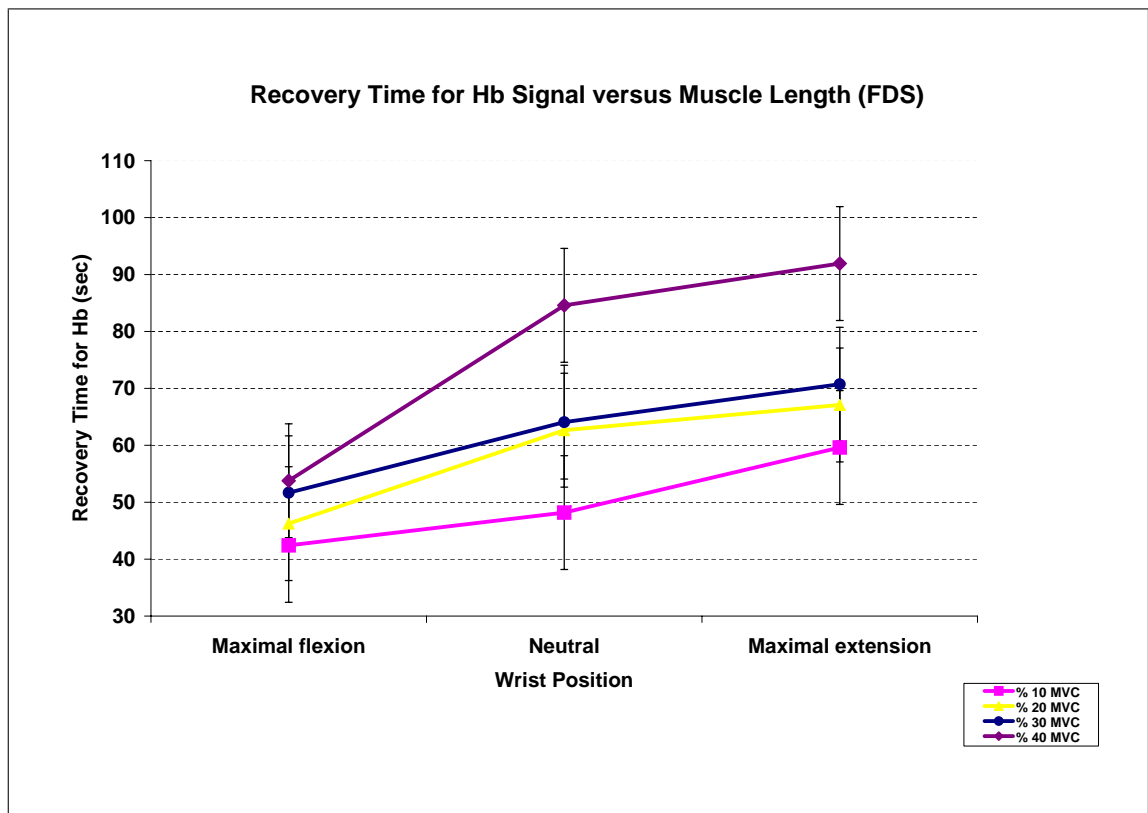


**Figure 5.4**  $t_{rec}$  at varying wrist positions for FDS muscle (data from Table 5.2).

When Figure 5.4 is analyzed, it is observed that (i)  $t_{rec}$  increases as the muscle

being probed is extended at a single contraction intensity and this result is observed for all contraction intensities, (ii)  $t_{rec}$  increases with increasing contraction intensity for all positions of the wrist.

### 5.3 Interpretation of Results

#### 5.3.1 The Relationship Between $mVO_2$ and the Level of Isometric Exercise

Our study illustrates that the increase in mean  $mVO_2$  of the subjects with incremental increase in exercise level is linear up to 40 % MVC. The linearity between  $mVO_2$  and the level of isometric exercise is in accordance with the findings from previous studies. Colier et al. reported a linear relationship between  $mVO_2$  in the soleus muscle and the level of isometric exercise expressed as % of MVC up to 20 % MVC [2]. Similarly; in a study by Van Beekvelt et al,  $mVO_2$  in the human FDS was evaluated during rhythmic isometric handgrip exercise in a range of work intensities. The increase in  $mVO_2$  was found to be closely related to the amount of work performed and the increase in  $mVO_2$  was linear up to 36 % MVC [31]. Also, Hamaoka et al. investigated changes in muscle  $O_2$  consumption with an increase in exercise intensity during submaximal isotonic grip exercise and found a linear relation up to 20 % MVC [37].

Quantitative measurement of  $mVO_2$  during exercise has been carried out by a few other groups [38, 31, 37, 2]. However, no comparison can be made with these studies because the exercise task and the muscle area of interest were substantially different. Another difficulty in obtaining comparable quantitative values from these studies was the discrepancy in the actual amount of work that was performed. But these studies also demonstrated a linearity between  $mVO_2$  and the level of isometric exercise which is in accordance with the findings of the present study.

$mVO_2$  at the onset of exercise gives an indication of local energy consumption since the energy consumption is dependent mainly on aerobic processes in this period. The increase in local energy consumption with increasing exercise intensity

during sustained handgrip exercise proves that the area being probed has a significant contribution to the flexion of the digits. The major function of FDS is to flex the interphalangeal and metacarpophalangeal joints of the second, third, fourth and fifth fingers [39]. The linear increase in  $mVO_2$  with increasing contraction intensity of the finger flexors during handgrip exercise strongly suggests that our measurements were taken from the superficial layer of FDS muscle which divides into tendons inserting in the middle and ring fingers.

The increase in local energy consumption with an increase in local force production can be related to the sliding filament theory of muscle contraction. According to the sliding filament theory, tension generated in a muscle fiber is directly proportional to the interaction between the thick and thin filaments. Consequently, the amount of force produced by a contracting muscle depends on the number of cross-bridges that are able to bind during contraction. Cross bridge dynamics together with the  $Ca^{+2}$  flow dynamics are the major energy consuming processes during contraction. Therefore; an increase in the number of cross-bridges attachments with an increase in contraction intensity results in higher energy consumption. Our study illustrates that  $mVO_2$  reflects the local energy consumption of the number of force-generating cross bridges assuming that the energy supply is mainly provided by aerobic metabolism. The results also imply that energy consuming processes during muscle contraction are linear processes up to 40 %MVC.

### 5.3.2 The Effect of Altering Wrist Position on $mVO_2$ of FDS Muscle

At a single contraction intensity,  $mVO_2$  of FDS muscle is observed to be lowest when the wrist is maximally extended.  $mVO_2$  of the area being probed increases when the wrist position is altered in favor of flexing the wrist flexors. As the plots of  $mVO_2$  at varying wrist positions are analyzed, it is observed that altering the wrist position has a substantial effect on the local energy consumption of FDS muscle.

Three conceptual explanations exist for such a position effect: (i) Length change

of FDS induced by wrist flexion/extension might have a significant influence on the local energy consumption. (ii) The more substantial length change of adjacent synergist muscles (FCU and FCR) may cause intermuscular myofascial force transmission to play a dominant role in regulating the net force produced by FDS muscle or (iii) the integrated effect of length and relative position changes of FDS, FCU and FCR might influence the energy cost of force production.

Muscles in the anterior compartment of the forearm work as a group and act to flex the wrist and the digits [39]. Flexor carpi radialis (FCR) and flexor carpi ulnaris (FCU) are the major flexors of the wrist. In assistance, FDS also contributes to the flexion of the wrist [39]. However, the extent of this contribution is not known and the sarcomere length change of FDS due to flexion and extension of the wrist has not been reported.

During sustained handgrip exercise, FDS muscle is flexed and has shorter length in comparison to its optimum length. Hence, the muscle being probed is in the ascending limb of the length tension curve. When the wrist is flexed maximally during handgrip task, FDS will be shortened and the sarcomeres will shift to a shorter length on the ascending limb of the length-tension curve. Inversely, when the wrist is extended maximally, FDS will be lengthened and the sarcomeres will shift to a longer length on the length-tension curve. The extent of such a shift in sarcomere lengths is not known but is considered to have a negligible effect on the force generating capacity of FDS. The noticeable effect of wrist position on local energy consumption of FDS can be explained by the changes in myotendinous force transmission to and from adjacent muscles.

Recent studies have shown that muscles transmit force not only through the myotendinous junction, but also through their intra-[40] and extra-muscular connections to adjacent structures [41]. This transmission of force outside the myotendinous junction is called myofascial force transmission. Animal experiments have shown that up to 37 % of muscle force may be transmitted to adjacent structures rather than reach the insertion of the muscle's tendon, and that the extent of such force transmission

depends on the length and relative position of these structures [42].

In a study by Yucesoy et. al. [43], the effects of inter- and extramuscular myofascial force transmission on muscle length-force characteristics were investigated. In that study, connective tissues at the bellies of the experimental synergistic muscles of the anterior crural compartment of rat were left intact. Extensor digitorum longus (EDL) was lengthened distally whereas tibialis anterior (TA) and extensor hallucis longus (EHL) muscles were kept at constant length. EDL was lengthened distally whereas tibialis anterior (TA) and extensor hallucis longus (EHL) were kept at constant muscle-tendon complex length. Distal EDL lengthening caused the distal force exerted by TA+ EHL complex to decrease to 17 % of the initial force. The result indicates increased myofascial force transmission from TA+ EHL complex to EDL muscle with distal lengthening of EDL [43].

The mechanical interaction of EDL and the TA+EHL complex can be seen as similar to the presently studied in-vivo condition of FDS, FCR and FCU during wrist extension. When the wrist is extended maximally, the length change of FDS muscle will be negligible in comparison to FCR and FCU. Extending the wrist maximally results in stretching of the individual muscle fibers of FCR and FCU to a greater extent. Smeulders et al. tested whether the force-length characteristics of human FCU varied with the change of relative length of adjacent muscles induced by a change in wrist position. The force-length characteristics of FCU were shown to change as a result of relative length differences with its surroundings and the results supported the idea that the contribution of myofascial force transmission depends on the mechanical conditions in which the muscle operates.

Altering the wrist position not only results in a length change in these muscles but also causes the position of the three muscles to change relative to each other which will affect the degree of intermuscular force transmission. Assuming that the force produced by FDS will be more severely influenced by changes in myofascial force transmission (rather than changes in absolute length of FDS), the lower  $m\dot{V}O_2$  observed during wrist extension may be related to the more substantial lengthening FCU and

FCR. It may be that as FCU and FCR are lengthened, force generated by FDS is likely to be transmitted via the myofascial pathway and add to the force of these synergistic muscles. Therefore; via the contribution of FDS to the external force being exerted may decrease which may be an explanation for lower energy consumption.

The mechanical interactions resulting in myofascial force transmission should influence energy consumption of the involved structures. In conditions in-vivo, the fraction of force that may be transmitted through the inter- and extramuscular connective tissue depends on muscle relative length and position. With a change in wrist position, the length of FCU and FCR and the extramuscular structures adjacent to FDS will be altered and the inter- and extra-muscular connections will be strained or relaxed. Such straining of connections may alter their stiffness and compliance [4]. However, direct measurement of active muscle force in humans have rarely been performed [41]. Depending on the relative compliance and the direction of pull of these connections, force generated by FDS may either be transmitted via the myofascial pathway or force exerted by adjacent structures may add to FDS force. The decrease in local  $m\dot{V}O_2$  of FDS muscle observed when the wrist position is altered in favor of extension may imply that force generated by FDS dissipates through the myofascial pathway to the adjacent muscles and/or connective tissues during maximal extension of the wrist. The relationship between  $m\dot{V}O_2$  and force level was shown to be linear up to 40 % MVC for the experimental design of our study. Hence; lower  $m\dot{V}O_2$  observed during maximal wrist extension suggests force generation by FDS was lower which may be due to increased myotendinous force transmission to adjacent structures.

### 5.3.3 The Relationship Between $t_{rec}$ and the Level of Isometric Exercise

The second parameter to be investigated was  $t_{rec}$ . Analyzing  $t_{rec}$  gives information about the degree of energy deficits accumulated in muscle during exercise as well as perfusion rate. Therefore; this parameter can be interpreted as an indicator of the amount of local energy consumption during exercise.  $t_{rec}$  reflects the reoxygenation profile of the muscle. However; it should be considered that the reoxygenation

rate is affected not only by the amount of  $O_2$  consumed during exercise but also by the availability of  $O_2$  delivery and uptake after occlusion is stopped. Blood flow in the exercising muscle is restricted during contractions because of the compression of capillaries as a result of increased intramuscular tissue pressure (IMP) [44].

$t_{rec}$  is prolonged when the exercise intensity (expressed as % MVC) is increased at a single wrist position. The restriction of blood flow to exercising muscle becomes more pronounced with an increase in exercise intensity. Prolonged  $t_{rec}$  observed with increasing exercise intensity is not only due to increased  $O_2$  deficiency but also due to an increase in compression of the capillaries which impedes blood perfusion after occlusion is ceased. Post-exercise oxygen delivery probably lags behind local oxygen consumption rate and the balance between  $O_2$  supply and uptake will be established in a longer time at higher work intensities.

Several studies have previously investigated post-exercise skeletal muscle oxygenation profiles with the aim of understanding the physiological response in terms of the energy cost incurred. The pioneering work of Chance et al. presented data regarding the changes in deoxygenation profile at incremental work intensities during rowing exercise. The resaturation times were found to increase with the intensity of work which is in accordance with the findings of the present study [24].

#### 5.3.4 The effect of altering wrist position on $t_{rec}$

$t_{rec}$  increases with increasing muscle length when the handgrip exercise is performed under similar percentages of MVC. This may be observed (i) due to increased  $O_2$  deficiency because of higher energy consumption or (ii) due to decreased post-exercise  $O_2$  delivery because of an increase in compression of the capillaries. Lengthening the muscle results in stretching of the individual muscle fibers and compression of the capillaries. An increase in IMP occurs which results in impaired blood flow.

Shorter  $t_{rec}$  observed during maximal flexion of the wrist may imply lower en-

ergy consumption during exercise. During the handgrip task, FDS is shorter than its optimum length. When the handgrip exercise is performed during maximal flexion of the wrist; FDS is further shortened and due to fewer crossbridge interactions; the area probed will contribute less to the total external force produced and consume less energy at a single exercise intensity. Consequently; the motor units which are detectable by the instrument may contribute less to the external force produced. However;  $t_{rec}$  is strongly affected by the amount of change in IMP during exercise. The increase in IMP may be less during maximally flexed position of the wrist in comparison to the maximally extended position. Therefore; the higher reoxygenation rate observed at shorter lengths may not truly reflect the local energy consumption during exercise.

Longer  $t_{rec}$  observed at longer muscle lengths suggests that the energy deficit accumulated during exercise was higher while the muscle is stretched which is in accordance with the hypothesis of lower energy consumption at shorter muscle lengths proposed by Fitch et. al.[45] . However; the fact that length dependent differences in internal muscle pressure contributed to differences in muscle perfusion cannot be neglected. In addition, blood flow could not be totally abolished during some of the experiments. The longer  $t_{rec}$  during maximal extension of the wrist may be due to higher energy deficit incurred during exercise but it may also be due to decreased  $O_2$  extraction capability of the tissue because of increased IMP. There are no existing studies that have attempted to analyze post-exercise time course of recovery at varying muscle lengths.

## 5.4 Limitations of the Study

In the present study, blood flow could not be totally occluded during some of the experiments. When changes in  $[HbO_2]$  and  $[Hb]$  are identical but in opposite directions, then  $mVO_2$  calculated from all signals will be identical. However, this situation can only be accomplished when blood volume stays constant during the occlusion, which is not always the case. An increase in total  $[Hb]$  ( $[Hb_{tot}]$ ) may occur not only due to incomplete arterial occlusion but also due to a redistribution of blood during the



occlusion. The increase in  $Hb_{tot}$  in some of the experiments resulted in a discrepancy between  $mVO_2$  calculated from  $[HbO_2]$  signal and that calculated from the OXY signal because the increase in  $[Hb]$  was no longer equal to the decrease in  $[HbO_2]$ . In cases where blood volume did not stay constant during exercise; it is not known whether the increase in blood volume originates from the arterial or venous site. Hence it is not known whether the extra volume contains mostly  $[Hb]$  or  $[HbO_2]$ . The true consumption of  $O_2$  may be reflected by a decrease in  $[HbO_2]$  but may also be reflected by an increase in  $[Hb]$ . OXY signal reflects the change in both  $[Hb]$  and  $[HbO_2]$ ; hence will prevent both over and under estimations of  $mVO_2$ . Consequently; OXY signal may be more reliable for measuring  $O_2$  consumption during exercise under arterial occlusion.

The work intensity of each exercise session was based on the individual maximum force production. However, the actual work intensity was less than the desired % of MVC because the force level at which subjects press on the hand dynamometer cannot be described by a perfect square waveform. The subjects couldnot endure holding the dynamometer with a constant force level in some of the experiments and this might lead to a discrepancy in the results.

Another limitation of the present study was the handicap in subject classification and inability to supply homogeneity in physical condition of the subjects. Such a handicap might have influence on the measurements and statistical results. One possible reason for highly varying metabolic rates (in terms of  $mVO_2$ ) were obtained at each exercise intensity may be the varying physiological and metabolic properties in the individuals.

## 5.5 Recommendations for Future Work

(i) The variability in  $mVO_2$  between subjects was reasonably high especially at the higher work intensities. Similar variation in  $mVO_2$  between subjects was found with Fick method at higher intensities [46]. The reason for this variability may be the

variation of physiological and metabolic properties of the subjects.

(ii) In some studies, the slopes of linear regression lines fitted to [Hb] and [HbO<sub>2</sub>] versus time curves at the onset of exercise were normalized to the maximal deoxygenation value. This was done to correct for local differences in subcutaneous fat under the optodes. Earlier studies have illustrated a negative linear relation between skinfold thickness and maximal deoxygenation which indicates that the measured mVO<sub>2</sub> depends on the kind of tissue below the optodes [47]. Maximal deoxygenation was demonstrated to be independent of local muscle length and force level [48]. Hence, it could be a good normalization parameter since its affect is only on mVO<sub>2</sub>. Adding a normalization parameter such as maximal deoxygenation could eliminate underestimations of mVO<sub>2</sub> due to local differences in subcutaneous fat layer thickness. However, the measurement site in their study was subject to significant variations in underlying adipose tissue layer thickness. In our study, the measurement site is not centered on a muscle where overlying skinfold thickness is substantial but for future work, skinfold thickness between the optodes and circumference of the forearm can be measured and used as a normalization parameter.

(iii) Subjects should be chosen to be of similar antropometric properties and attention should be paid to homogeneity in physical conditions of the subjects while the experiments are performed.

## 6. CONCLUSION

This study was performed to analyze the relationship between local energy consumption and local force generation under varying biomechanical conditions with NIRS. Nine subjects participated in the study. Sustained handgrip exercise was performed at four different force levels for three different wrist positions with the aim of understanding the effect of muscle absolute length and relative position changes on local energy consumption and local force production.

mVO<sub>2</sub> increased linearly with exercise level and this result was observed while the wrist was maximally flexed, maximally extended and in neutral position. At each exercise level, mVO<sub>2</sub> is observed to be lowest while the wrist is maximally extended. It is concluded that changing relative position and absolute length of FDS muscle and its adjacent synergist muscle affects the degree of force transmission among these structures which directly influences the net force produced by FDS. The direction of force transmission is not known but it is suggested that during maximal extension, part of the force generated by FDS is transmitted to FCR and FCU which causes a decrease in FDS force. The lower energy consumption observed during maximal extension may imply lower force generation by FDS.

$t_{rec}$  was also analyzed as a measure of O<sub>2</sub> deficiency incurred during exercise.  $t_{rec}$  increased with increasing force level at all wrist positions. Under the same contraction intensity,  $t_{rec}$  increased as the exercise was performed at longer lengths of FDS. However,  $t_{rec}$  is a controversial parameter because the reoxygenation profile is strongly affected by the amount of increase in IMP during exercise. Hence; it does not truly reflect the energy consumption during exercise. Nevertheless; the increase in  $t_{rec}$  with an increase in force level indicates that the balance between post-exercise O<sub>2</sub> delivery and uptake will be established in a longer time (i) because of increased energy deficits and (ii) increased IMP which impedes blood perfusion after occlusion is ceased.

These results imply that local energy consumption increases linearly with force level and energy consuming processes during muscle contraction are most likely to be linear processes up to 40 %MVC. Myofascial force transmission between a muscle and its adjacent structures is thought to affect the local force generating capacity and may be a co-determinant of local energy consumption during force generation. The study shows that local muscle oxygen consumption can be measured reliably with NIRS during exercise in a range of work intensities. This is of great importance because direct local measurement of  $m\dot{V}O_2$  is not possible with the conventional techniques. The study also shows that NIRS is a promising tool for understanding muscle physiology as it can give more insight to the regulation of local tissue oxygenation in normal physiological situations and during exercise.

## APPENDIX A. $mVO_2$ and $t_{rec}$ Values for the Whole Set of Experiments

**Table A.1**  
 $mVO_2$  values measured from the Hb signal

<b><math>mVO_2</math> (Hb)</b>				
<b>Activity</b>	<b>Subjects</b>	<b>Neutral</b>	<b>Flexion</b>	<b>Extension</b>
<b>% 10 MVC</b>	<b>1</b>	0.17	0.21	0.04
	<b>2</b>	0.29	0.21	0.15
	<b>3</b>	0.15	0.38	0.27
	<b>4</b>	0.10	0.13	0.09
	<b>5</b>	0.21	0.24	0.14
	<b>6</b>	0.12	0.26	0.12
	<b>7</b>	0.69	0.16	0.37
	<b>8</b>	0.16	0.18	0.05
	<b>9</b>	0.19	0.68	0.10
<b>% 20 MVC</b>	<b>1</b>	0.50	0.38	0.16
	<b>2</b>	0.23	0.26	0.15
	<b>3</b>	0.23	0.40	0.21
	<b>4</b>	0.12	0.14	0.11
	<b>5</b>	0.13	0.34	0.12
	<b>6</b>	0.25	0.24	0.24
	<b>7</b>	0.64	0.44	0.43
	<b>8</b>	0.12	0.45	0.10
	<b>9</b>	0.15	0.22	0.20
<b>% 30 MVC</b>	<b>1</b>	0.60	0.62	0.41
	<b>2</b>	0.49	0.62	0.62
	<b>3</b>	0.53	0.29	0.11
	<b>4</b>	0.19	0.10	0.12
	<b>5</b>	0.15	0.39	0.25
	<b>6</b>	0.37	0.18	0.31
	<b>7</b>	0.28	0.66	0.36
	<b>8</b>	0.15	0.18	0.12
	<b>9</b>	0.34	0.69	0.11
<b>% 40 MVC</b>	<b>1</b>	1.02	0.76	0.99
	<b>2</b>	0.21	0.68	0.13
	<b>3</b>	0.13	0.59	0.60
	<b>4</b>	0.63	0.23	0.13
	<b>5</b>	0.23	0.54	0.33
	<b>6</b>	0.44	0.45	0.48
	<b>7</b>	0.35	0.60	0.45
	<b>8</b>	0.47	0.15	0.22
	<b>9</b>	0.41	0.33	0.14
<b>p value</b>	<b>Rows</b>	<b>0.0020</b>		
	<b>Columns</b>	<b>0.0004</b>		

**Table A.2**  
 $t_{rec}$  measured from the Hb signal.

Activity	T rec (Hb)			
	Subjects	Neutral	Flexion	Extension
% 10 MVC	1	25.84	26.18	48.501
	2	28.66	22.17	62.41
	3	46.53	51.26	54.11
	4	51.76	43.04	153.38
	5	91.65	47.20	70.271
	6	55.63	36.97	37.784
	7	51.90	34.63	30.20
	8	39.29	27.82	38.24
	9	42.37	92.51	41.59
% 20 MVC	1	68.17	35.70	160.76
	2	70.21	32.92	40.10
	3	74.55	28.14	42.245
	4	52.39	32.05	41.47
	5	55.53	64.40	53.723
	6	74.70	33.40	38.83
	7	53.01	66.07	149.20
	8	35.68	81.70	23.46
	9	79.64	41.80	53.977
% 30 MVC	1	78.46	47.73	40.31
	2	78.46	43.36	46.68
	3	57.22	47.02	163.33
	4	88.39	38.74	69.31
	5	42.79	124.47	53.72
	6	29.36	23.05	47.07
	7	36.82	48.02	69.63
	8	76.68	24.07	71.94
	9	88.39	68.49	74.62
% 40 MVC	1	83.165	54.14	66.79
	2	80.54	31.23	68.46
	3	116.19	47.89	103.71
	4	72.68	51.92	88.45
	5	162.60	66.65	66.70
	6	24.26	58.19	182.26
	7	80.14	62.07	151.97
	8	38.84	44.49	38.33
	9	102.84	67.37	60.70
p value	Rows	0.0060		
	Columns	0.0230		

## REFERENCES

1. Rassier, D. E., B. R. MacIntosh, and W. Herzog, "Length dependence of active force production in skeletal muscle," *Journal of Applied Physiology*, Vol. 86, pp. 1445–1457, 1999.
2. Colier, W. N., I. B. Meeuwsen, H. Degens, and B. Oesburg., "Determination of oxygen consumption in muscle during exercise using near infrared spectroscopy," *Acta Anaesthesiol Scand*, Vol. 39 (Suppl 107), pp. 151–155, 1995.
3. Praagman, M., H. E. J. Veeger, E. K. J. Chadwick, W. N. J. M. Colier, and F. C. T. van der Helm, "Muscle oxygen consumption, determined by nirs, in relation to external force and emg.," *J Biomech*, Vol. 36, pp. 905–912, Jul 2003.
4. Huijing, P. A., and G. C. Baan, "Myofascial force transmission: muscle relative position and length determine agonist and synergistic muscle force," *Journal of Applied Physiology*, Vol. 94, pp. 1092–1107, 2003.
5. W D Mc.Ardle, F I Katch, V. L. K., *Exercise Physiology: Energy Nutrition and Performance*, ch. Chapter 18, pp. 359–381. Williams & Wilkins Publishers, 2001.
6. Silverthorn, D. U., *Human Physiology: An Integrated Approach*, Daryl Fox, 2003.
7. Gordon, A. M., A. F. Huxley, and F. J. Julian., "The variation in isometric tension with sarcomere length in vertebrate muscle fibres," *Journal of Physiology (London)*, Vol. 184, pp. 170–192, 1966.
8. Huxley, A. F., and R. M. Simmons, "Proposed mechanism of force generation in striated muscle," *Nature*, Vol. 233, pp. 533–538, 1971.
9. Godt, R. E., and D. W. Maughan., "Influence of osmotic compression on calcium activation and tension in skinned muscle fibers of the rabbit.," *Pflügers Arch.*, Vol. 391, pp. 334–337, 1981.
10. Sato, T. G., "Volume changes of muscle fiber on tetanic contractions," *Annothes. Zoology*, Vol. 27, pp. 165–172, 1954.
11. Herzog, W., S. Kamal, and H. D. Clarke., "Myofilament lengths of cat skeletal muscle: theoretical considerations and functional implications," *Journal of biomechanics*, Vol. 25, pp. 945–948, 1992.

12. Yucesoy, C. A., B. H. F. J. M. Koopman, H. J. Grootenboer, and P. A. Huijing, "Extramuscular myofascial force transmission : Experiments and finite element modeling," *Archives of Physiology and Biochemistry*, Vol. 111, pp. 317–388, 2005.
13. Jöbsis, F. F., "Non-invasive infrared monitoring cerebral and myocardial oxygen sufficiency and circulatory parameters," *Science*, Vol. 198, pp. 1264–1267, 1977.
14. Ferrari, M., T. Binzoni, and V. Quaresima, "Oxidative metabolism in muscle," *Phil. Trans. R. Soc. Lond. B*, Vol. 352, pp. 667–683, 1997.
15. Ferrari, M., L. Mottola, and V. Quaresima, "Principles, techniques, and limitations of near infrared spectroscopy," *Can J Appl Physiol.*, Vol. 29, pp. 463–487, 2004.
16. Quaresima, V., R. Lepanto, and M. Ferrari, "The use of near infrared spectroscopy in sports medicine," *Journal of Sports Medicine and Physical Fitness.*, Vol. 43, pp. 1–13, 2003.
17. Manchini, D. M. L., H. Bolinger, K. Li, and B. Chance, "Validation of near infrared spectroscopy in humans," *Journal Of Applied Physiology*, Vol. 77, pp. 2740–2747, 1994.
18. Belardinelli, R., T. J. Barstow, J. Porszasz, and K. Wasserman, "Changes in skeletal muscle oxygenation during incrementalexercise measured with near infrared spectroscopy," *European Journal Of Applied Physiology*, Vol. 70, pp. 487–492, 1995.
19. Delpy, D. T., and M. Cope., "Estimation of optical pathlength through tissue from direct time of flight measurement," *Phys. Med. Biol.*, Vol. 33, pp. 1433–1442, 1988.
20. Blasi, R. A. D., M. Ferrari, A. Natali, G. Conti, A. Mega, and A. Gasparetto, "Non-invasive measurement of forearm blood flow and oxygen consumption by near infrared spectroscopy," *J. Appl. Physiol.*, Vol. 76, pp. 1388–1393, 1994.
21. Alkas, E., "Quantification of the effect of warm up and stretching on the oxygen metabolism using an improved version of a fnirs device," Master's thesis, Boğaziçi University, 2003.
22. Gulsoy, M., *Optical properties of biological tissue*. Boğaziçi University, BM 585 lecture notes.
23. Takaishi, T., T. Sugiura, K. Katayama, Y. Sato, Y. Shima, N. Yamamoto, and T. Moritani, "Changes in blood volume and oxygenation level in a working muscle during a crank cycle," *Med. Sci. Sports Exerc*, Vol. 33, pp. 520–528, 2002.



24. Chance, B., M. T. Dait, C. Zhang, T. Hamaoka, and F. Hagerman., "Recovery from exercise-induced desaturation in the quadriceps muscles of elite competitive rowers.," *American Journal Of Physiology.*, Vol. 262, pp. C776–C775, 1992.
25. Quaresima, V., W. N. Colier, M. V. der Slujs, and M. Ferrari., "Nonuniform quadriceps oxygen consumption revealed by near infrared multipoint measurements.," *Biochem Biophys Res Commun.*, Vol. 285, pp. 1034–1039, 2001.
26. Nioka, S., H. Miura, H. Long, A. Pecry, D. Moser, and B. Chance, "Functional quadriceps and gastrocnemius imaging in elite and untrained subjects," in *Proc SPIE*, 1999.
27. Hampson, N. B., and C. A. Piantadosi, "Near infrared monitoring of human skeletal muscle oxygenation during forearm ischemia," *Journal of Applied Physiology*, Vol. 64, pp. 2449–2457, 1988.
28. Cheatle, T. R., L. A. Potter, M. Cope, D. T. Delpy, P. D. Smith, and J. H. Scurr, "Near-infrared spectroscopy in peripheral vascular disease," *British Journal of Surgery*, Vol. 78, pp. 405–408, 1991.
29. Hamaoka, T., H. Iwane, T. Shimomitsu, T. Katsumura, N. Murase, and S. Nishio, "Non-invasive measures of oxidative metabolism on working human muscles by near-infrared spectroscopy," *J Appl Physiology*, Vol. 81, pp. 1410–1417, 1996.
30. T. Sako, T. Hamaoka, H. H. Y. K., and T. K. ., "Validity of nir spectroscopy for quantitatively measuring muscle oxidative metabolic rate in exercise.," *Journal of Applied Physiology.*, Vol. 90, pp. 338–344., 2001.
31. Beekvelt, M. C. V., W. N. Colier, R. A. Wevers, and B. G. V. Engelen., "Performance of near-infrared spectroscopy in measuring local oxygen consumption and blood flow in skeletal muscle.," *Journal of applied Physiology.*, Vol. 90, pp. 511–519., 2001.
32. Homma, S., H. Eda, S. Ogasawara, and A. Kagaya, "Near-infrared estimation of oxygen supply and consumption in forearm muscles working at varying intensity," *J Appl Physiology*, Vol. 80, pp. 1279–1284, 1996.
33. Kasikcioglu, E., A. Arslan, B. Topcu, O. Sayli, H. Akhanc, H. Oflaz, A. Akin, A. Kayserilioglu, and M. Meric., "Cardiac fatigue and oxygen kinetics after prolonged exercise," *International Journal of Cardiology*, Vol. 108, pp. 286–288, 2005.

34. Binzoni, T., W. Colier, E. Hiltbrand, D. L. Hoof, and P. Cerretelli, "Muscle oxygen consumption by nirs: a theoretical model," *Journal of Applied Physiology*, Vol. 87, pp. 683–688, 1999.
35. Emir, U. A., "System characterization for a fast optical imager.," Master's thesis, Boğaziçi University, 2003.
36. Cheatle, T. R., L. A. Potter, M. Cope, D. T. Delpy, P. D. C. Smith, and J. H. Scurr., "Near-infrared spectroscopy in peripheral vascular disease.," *British Journal of Surgery*, Vol. 78, pp. 405–408, 1991.
37. Hamaoka, T., H. Iwane, T. Shimomitsu, T. Katsumura, N. Murase, and S. Nishio., "Non-invasive measures of oxidative metabolism on working human muscles by near-infrared spectroscopy," *Journal of Applied Physiology*, Vol. 81, pp. 1410–1417, 1996.
38. R. A. De Blasi, M. Ferrari, A. N. G. C. A. M., and A. Gasparetto., "Noninvasive measurement of forearm blood flow and oxygen consumption by near infrared spectroscopy," *Journal of Applied Physiology*, Vol. 76, pp. 1338–1393., 1994.
39. Jenkins, W. G., C. P. Kemnitz, and G. J. Tortora, *Anatomy and Physiology*, ch. Chapter 11, pp. 380–386. John Wiley & Sons, Inc, 1999.
40. Huijing, P. A., and G. C. Baan, "Muscle as a collagen fiber reinforced composite: a review of force transmission in muscle and whole limb," *Journal of Biomechanics*, Vol. 32, pp. 329–345, 1999.
41. Mendelson, L. S., P. H. Peckham, A. A. Freehafer, and M. W. Keith, "Intraoperative assessment of wrist extensor muscle force.," *Journal of Hand Surgery*, Vol. 13, pp. 832–836, 1988.
42. Smeulders, M. J. C., M. Kreulen, J. Hage, P. A. Huijing, and C. M. A. M. V. der Horst., "Spastic muscle properties are affected by length changes of adjacent structures," *Muscle Nerve*, Vol. 32, pp. 208–215, 2005.
43. Yucesoy, C. A., B. H. F. J. M. Koopman, G. C. Baan, H. J. Grootenboer, and P. A. Huijing, "Effects of inter- and extramuscular myofascial force transmission on adjacent synergistic muscles: assessment by experiments and finite-element modeling," *Journal of Biomechanics*, Vol. 36, pp. 1797–1811, 2003.

44. Yamada, E., T. Kusaka, K. Miyamoto, S. Tanaka, S. Morita, S. Tanaka, Y. Cao, S. Mori, H. Norimatsu, and S. Itoh, "Relationships between changes in oxygenation during exercise and recovery in trained athletes.," *Optical Review*, Vol. 10, pp. 436–439, 2003.
45. S, F., and M. A., "Influence of human muscle length on fatigue.," *Journal of Physiology*, Vol. 362, pp. 205–213, 1985.
46. Hartling, O. J., H. Kelbaek, T. Gjorup, B. Schibye, K. Klausen, and T. J. J., "Forearm oxygen uptake during maximal forearm dynamic exercise," *European Journal of Applied Physiology*, Vol. 58, pp. 446–470, 1989.
47. Beekvelt, M. C. V., M. S. Borghuis, B. G. van Engelen, R. A. Wevers, and W. N. Collier, "Adipose tissue thickness affects in vivo quantitative near-ir spectroscopy in human skeletal muscle.," *Clin Sci (Lond)*, Vol. 101, pp. 21–28, 2001.
48. de Ruiten, C. J., M. D. de Boer, M. Spanjaard, and A. de Haan, "Knee angle-dependent oxygen consumption during isometric contractions of the knee extensors determined with near-infrared spectroscopy," *Journal of applied Physiology*, Vol. 99, pp. 579–586, 2004.